Shape coexistence in the odd-odd nucleus ^{98}Y: The role of the $g_{9/2}$ neutron extruder

W. Urban,[1] M. Czerwiński,[1] J. Kurpeta,[1] T. Rząca-Urban,[1] J. Wiśniewski,[1] T. Materna,[2] Ł. W. Iskra,[3] A. G. Smith,[4] I. Ahmad,[5] A. Blanc,[6] H. Faust,[6] U. Köster,[6] M. Jentschel,[6] P. Mutti,[6] T. Soldner,[6] G. S. Simpson,[7] J. A. Pinston,[7] G. de France,[8] C. A. Ur,[9] V.-V. Elomaa,[10] T. Eronen,[10] J. Hakala,[10] A. Jokinen,[10] A. Kankainen,[10] I. D. Moore,[10] J. Rissanen,[10] A. Saastamoinen,[10] J. Szerypo,[10] C. Weber,[10] and J. Äystö[10]

[1]*Faculty of Physics, University of Warsaw, ulica Pasteura 5, PL-02-093 Warsaw, Poland*
[2]*IRFU, CEA, DSM-Saclay, F-91191 Gif-sur-Yvette, France*
[3]*Institut of Nuclear Physics, PAN, 31-342 Kraków, Poland*
[4]*Department of Physics and Astronomy, The University of Manchester, M13 9PL Manchester, United Kingdom*
[5]*Argonne National Laboratory, Argonne, Illinois 60439, USA*
[6]*Institut Laue-Langevin, 71 Avenue des Martyrs, F-38042 Grenoble Cedex, France*
[7]*Laboratoire de Physique Subatomique et de Cosmologie, IN2P3-CNRS/Université Grenoble Alpes, F-38026 Grenoble Cedex, France*
[8]*Grand Accélérateur National d'Ions Lourds (GANIL), CEA/DSM - CNRS/IN2P3, Bd Henri Becquerel, BP 55027, F-14076 Caen Cedex 5, France*
[9]*INFN, Legnaro, Italy*
[10]*Department of Physics, University of Jyväskylä, P.O. Box 35 (YFL), FI-40014 Jyväskylä, Finland*

(Received 9 May 2017; revised manuscript received 8 September 2017; published 30 October 2017)

Excited states in ^{98}Y, populated in neutron-induced fission of ^{235}U and in spontaneous fission of ^{248}Cm and ^{252}Cf, have been studied by means of γ spectroscopy using the Lohengrin fission-fragment separator at ILL Grenoble and the EXILL, Eurogam2, and Gammasphere Ge arrays. Two new isomers have been found in ^{98}Y: a deformed one with $T_{1/2} = 180(7)$ ns and a rotational band on top of it, and a spherical one with $T_{1/2} = 0.45(15)$ μs, analogous to the 8^+ isomer in ^{96}Y, corresponding to the $(\nu g_{7/2}, \pi g_{9/2})_{8^+}$ spherical configuration. Using the JYFLTRAP Penning trap, an accurate excitation energy of 465.7(7) keV has been determined for the 2.36-s isomer in ^{98}Y. This result and the studies of excited levels in ^{98}Zr, populated in β^- decay of the isomer, indicate a new spin-parity, $I^\pi = (7)^+$ for the isomer. The high spin and the decay properties of this isomer suggest the presence of the $9/2^+[404]$ neutron extruder orbital in its structure. This is consistent with the large deformation of the isomer, reported recently. The present work does not provide arguments to support the special role of the $\nu g_{7/2}$ - $\pi g_{9/2}$ interaction (the spin-orbit-partner, or SOP, mechanism).

DOI: 10.1103/PhysRevC.96.044333

I. INTRODUCTION

In the chain of neutron-rich yttrium isotopes, the ground state of the ^{96}Y nucleus is nearly spherical while in ^{100}Y it is strongly deformed. The transitional nucleus ^{98}Y, located between the two, at the $N = 59$ neutron line, the pivotal border between spherical and well deformed nuclei in the $A \sim 100$ region, is an extraordinary example of the shape coexistence. Experimental studies of this particular nucleus are of great importance for testing mechanisms producing nuclear deformation.

As discussed in Ref. [1], in this region the deformed minimum in the nuclear potential is primarily due to the population of the "deformation driving" low-Ω subshells of the neutron intruder orbital $\nu h_{11/2}$, [2,3] helped by vacating the $\nu 9/2[404]$ extruder [4,5]. At the same time a spherical minimum is preserved in these isotopes up to $N = 60$, due to the $Z = 38$ and $Z = 40$ subshell closures. The competition of both minima gives rise to the famous "sudden" onset of deformation at $N = 59$ (see Fig. 8 in Ref. [6] and Refs. [1,7]). In this picture the $\nu 9/2[404]$ plays a special, double role, first stabilizing the spherical shape until the deformed minimum achieves a deformation sufficient to elevate this orbital to the Fermi level and then stabilizing the deformed minimum, at higher deformation. Therefore, experimental investigations of this orbital are of prime importance. To date it has not been observed in ^{98}Y or in any other odd-odd nucleus.

The proximity of the spherical and deformed minima in ^{98}Y allows tunneling between them, which gives rise to rich isomerism in this nucleus. As discussed in Ref. [8], the 1180-keV, $T_{1/2} = 0.72$ μs isomer in ^{98}Y is due to the $(\pi g_{9/2}, \nu h_{11/2})_{10^-}$ spherical configuration, which decays to the $(\pi 5/2^+[422], \nu 3/2^-[541])_{4^-}$ deformed structure, originating from the same $\pi g_{9/2}$ and $\nu h_{11/2}$ orbitals. A similar effect is seen in ^{96}Rb [8] and, as pointed out in Ref. [8], the $N = 59$ line may be the unique place in the nuclear chart where such a phenomenon occurs.

As there are more deformation-driving orbitals near the Fermi level in ^{98}Y, other deformed configurations may be expected, influencing the evolution of deformation in the region and, eventually, decaying to some spherical counterparts via isomeric transitions. Of particular interest is the structure of the 2.36-s, β^--decaying isomer in ^{98}Y, for which the largest deformation of all yttrium isotopes has been reported [9].

Finally, recent works [10,11] suggest that the emergence of the deformation around $N = 59$ in even-even Zr isotopes is connected with a significant rearrangement of nuclear shells, the effect called type II shell evolution. Such a rearrangement should leave clear signatures in the structure of the odd-A and, in particular, odd-odd neighboring nuclei. The study of

odd-odd yttrium isotopes may thus serve as a sensitive tool for testing this newly proposed deformation-driving mechanism.

In this work we report on an experimental study of low-to-medium-spin levels in the ^{98}Y nucleus. Our goal was to search for new configurations, both spherical and deformed. Furthermore, because for many levels in ^{98}Y their spin-parity assignments are still uncertain [12], we also verified the existing information on spins and parities and proposed new assignments, crucial for the interpretation of the observed configurations, in particular concerning the 2.36-s isomer. To help this we studied, in addition, β^- decays of both the ground state and the 2.36-s isomer in ^{98}Y to levels in ^{98}Zr.

Section II of this work presents the experiments performed in this work. In Sec. III we describe the data analysis and the results of our measurements. In Sec. IV the experimental data are discussed and compared to calculations. Section V summarizes the work.

II. EXPERIMENTS PERFORMED TO STUDY ^{98}Y AND ^{98}Zr NUCLEI

In order to study ^{98}Y and ^{98}Zr nuclei we used the data from seven experiments. Motivations for these measurements and the techniques used are briefly presented below. To facilitate the reading, we labeled these experiments as Exp. 1 to Exp. 7 in the text.

A. Measurement of prompt-γ rays from spontaneous fission of ^{248}Cm (Exp. 1)

New medium-spin excitations in ^{98}Y were searched for by analyzing triple-γ coincidences between prompt-γ rays emitted by fission fragments populated in spontaneous fission of ^{248}Cm. The γ radiation was measured using the Eurogam2 array of anti-Compton spectrometers [13]. In the measurement about 2.5×10^9 high-fold coincidences were collected. The electronic time-coincidence window was 400 ns, counted from the "start" given by the "master-gate" signal (for more details on the experiment and data analysis techniques see Refs. [14–16]).

In spontaneous fission of ^{248}Cm prompt-γ rays deexciting levels in ^{98}Y are in time coincidence with prompt-γ rays deexciting levels in ^{147}La, the most abundant fission-fragment partner to ^{98}Y. Gating on the well known γ lines of ^{147}La [17] greatly facilitated the search for new excitations in ^{98}Y.

B. Measurement of prompt-γ rays from spontaneous fission of ^{252}Cf (Exp. 2)

The results from the measurement of ^{248}Cm fission, have been verified and extended in a measurement of γ rays following spontaneous fission of ^{252}Cf, performed using the Gammasphere array of Ge detectors at Argonne National Laboratory (see Ref. [18] for more information on the experiment). In the measurement about 1.2×10^{11} triple coincidences were collected, an order of magnitude more than in the measurement of ^{248}Cm fission. The electronic time-coincidence window of 900 ns, counted from the "start" given by the "master-gate" signal, was factor of 2 longer than in the ^{248}Cm fission measurement. Good timing of the ^{252}Cf data provided accurate half-lives in the nano- to microsecond range and an effective use of the delayed coincidences for cleaning γ spectra.

Despite these advantages of the ^{252}Cf experiment, the ^{248}Cm fission measurement was analyzed first to identify new lines in ^{98}Y, because the ^{152}Pr nucleus, which is the most abundant complementary fragment to ^{98}Y, has a complex and poorly known excitation scheme.

C. Search for new isomers in ^{98}Y in the time range of seconds (Exp. 3)

Some open questions about the 2.36-s isomer ^{98}Y, prompted us to look for other possible isomers in ^{98}Y, especially in the seconds time range. In this context it is also of interest to verify the properties of β^- -decay of both the ground state and the 2.36-s isomer of ^{98}Y as well as β^- decay of the ground state of ^{98}Sr. Therefore we measured γ and β radiations emitted by mass $A = 98$ ions populated in neutron-induced fission of ^{235}U and separated using the Lohengrin fission-fragment separator [19] equipped with an electrostatic deflector.

The detection setup consisted of an ionization chamber, three Ge detectors (two clovers and a GammaX) placed around the chamber, and a β detector located in front of the chamber.

To search for new isomers in the second range we used the electrostatic deflector of Lohengrin operating at the frequency of 0.005 Hz. The cycle of the deflector was 90 s "beam ON" followed by 110 s "beam OFF." In the measurement we collected about 3×10^7 ions. The ions were not removed from the measurement point.

D. Search for new isomers in ^{98}Y in the micro- to milliseconds time range (Exp. 4)

Because at Lohengrin the ions arrive to the collection point about 1.7 μs after being produced in thermal-neutron-induced fission of an actinide target inside the ILL reactor, we could observe isomers with half-lives from a fraction of a microsecond up.

To search for new isomers in the micro- to millisecond range we used the electrostatic deflector of Lohengrin, operating at a frequency of 100 Hz (for more details see Ref. [20]). The cycle of the deflector was 6 ms "beam ON" followed by 4 ms "beam OFF." The start signal for the time measurement was provided by the deflector. The digital acquisition system running with a 40 MHz clock provided the possibility to measure half-lives in the microsecond range, using as the start the precise time signal from the ionization chamber. The detection setup was the same as in Exp. 3. In the measurement performed at this frequency about 6×10^7 ions were collected. The ions were not removed from the measurement point.

E. Measurements of low-spin excitations in ^{98}Y and ^{98}Zr (Exp. 5)

Population of some levels in ^{98}Y in the β^- decay of ^{98}Sr differs between various works reported previously. For the 1^+ level at 600.2 keV the population changed from 80% [21] to 67% [22] and then to 42% in the compilation [12], which includes the unpublished data [23]. Also intriguing is

the 0.22% population of the 496.1-keV level in β^- decay of the 0^+ ground state of ^{98}Sr [12].

To verify these numbers we measured properties of levels in ^{98}Y populated in β^- decay of ^{98}Sr, using the Lohengrin separator. The detection setup consisted of two clover detectors on both sides of the chamber and three β detectors around the chamber. The mass $A = 98$ ions arriving to the detection point were deposited on a tape and periodically removed to limit the background due to long-lived decays. The tape movement was correlated with the cycle of the Lohengrin deflector of 8 s "beam ON" followed by 8 s "beam OFF." The measurement was performed over the first 16 seconds of the cycle. During the following 2 seconds the tape was moved. Using the digital acquisition system, running with a 40 MHz clock, we collected about 9×10^7 γ time signals and about 5×10^6 β time signals registered within a 600 ns hardware time window started by a γ signal.

F. Multipolarity measurements of γ transitions in ^{98}Y and ^{98}Zr (Exp. 6)

To find spins and parities of crucial excitations in ^{98}Y and ^{98}Zr, we analyzed angular correlations and directional-polarization correlations for cascades of γ rays in both nuclei observed following the neutron-induced fission of ^{235}U. The measurement was performed at the cold-neutron facility PF1b at the research reactor of ILL Grenoble. We used the EXILL array, containing eight large EXOGAM [24] clover detectors arranged in an octagonal geometry, enabling precise angular correlation and directional-polarization correlation measurements (for the description of the EXILL experiment see also Refs. [25–27]). For the polarization sensitivity calibration of the EXOGAM clovers we took the energy dependence of the sensitivity calibration as reported in Refs. [24,28] for the EXOGAM and Eurogam clover detectors, respectively, and normalized it using the characteristic known $0^+ \rightarrow 2^+ \rightarrow 0^+$ cascades observed in the present EXILL data.

G. Measurement of the excitation energy of the 2.36-s isomer in ^{98}Y (Exp. 7)

Because of some inconsistency between the spin of the known 2.36-s isomer in ^{98}Y, its excitation and decay properties, reported previously [29,30], we remeasured the mass of the 2.36-s isomer using the JYFLTRAP Penning trap at Jyväskylä University. The detailed description of the technique is given in Ref. [31].

The Ramsey cleaning method was used to prepare isomerically pure samples of either the ground state or the isomeric state of ^{98}Y [32]. In total, three time-of-flight ion cyclotron resonance curves were obtained for ^{98m}Y and four for the ^{98}Y ground state using Ramsey's technique of time-separated oscillatory fields [33]. Count-rate-class analysis [34] showed that the curve fits did not suffer from ion number dependent frequency shifts.

III. DATA ANALYSIS AND RESULTS

In this section we present the results for excited levels in ^{98}Y, for excited levels in ^{98}Zr and for the 2.36-s isomer in ^{98}Y, obtained from the analysis of Exp. 1 – Exp. 7.

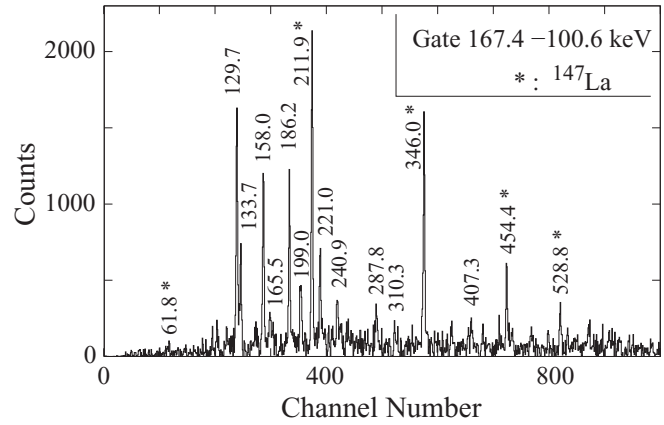

FIG. 1. γ spectrum doubly gated on the 167.4-keV line of ^{147}La and the 100.6-keV line of ^{98}Y, obtained from a histogram of triple-γ coincidences from fission of ^{248}Cm.

A. Excited levels of ^{98}Y

1. *Medium-spin excited levels of ^{98}Y*

Figure 1 shows a γ spectrum cut from a 3D histogram containing prompt triple-γ coincidences from the ^{248}Cm fission data, sorted within a 400-ns time window. The spectrum is gated on the 167.4-keV line of ^{147}La and the known 100.6-keV line in the band on top of the 8.95-μs isomer at 496.1-keV in ^{98}Y [12]. In the spectrum one can see prompt-γ lines of this band and of ^{147}La. This and other gated spectra support band 1 shown in Fig. 2, which was reported in Ref. [36] and extended recently to spin $I = 12$ [37].

A γ spectrum displayed in Fig. 3, which is doubly gated on the known, 204.3- and 228.6-keV lines of ^{98}Y [36], shows the 265.9- and 313.9-keV lines reported previously [36], and new lines at 54.7 and 449.5 keV, which are arranged into an irregular band of spherical excitations, drawn as band 2 in Fig. 2. The intensity balance in the cascade provided the estimate of the total conversion coefficient for the 54.7-keV transition, $\alpha_{\rm tot}(54.7) = 1.5(2)$, indicating that this is an $M1$ transition with a small admixture of $E2$. Based on the observed intensities, we placed the 54.7-keV transition below the 313.9-keV transition, changing the position of the latter reported in Ref. [36].

From the data of Exp. 5 we have sorted a three-dimensional (3D) histogram of triple-γ events in a 600-ns time window to search for new, weak effects which may show up thanks to a low background in this measurement. In Fig. 4 we show the low-energy fragment of a γ spectrum, which is the sum of γ spectra obtained from the $\gamma\gamma\gamma$ cube by setting double gates on all pairs of γ lines in the 204.3-228.6-54.7-313.9-keV cascade of ^{98}Y. The spectrum indicates that the cascade must be populated in a decay of an isomer, arriving at the detection point of Lohengrin in an excited state, after being produced in the fission of ^{235}U in the target. As no link between the 971.3-keV level and the 1181.4-keV isomer could be identified, we propose that the 971.3-keV level corresponds to a new isomer in ^{98}Y.

We note that, to date, the highest excitation energy ^{98}Y observed in fission [37] is at least two times lower than that

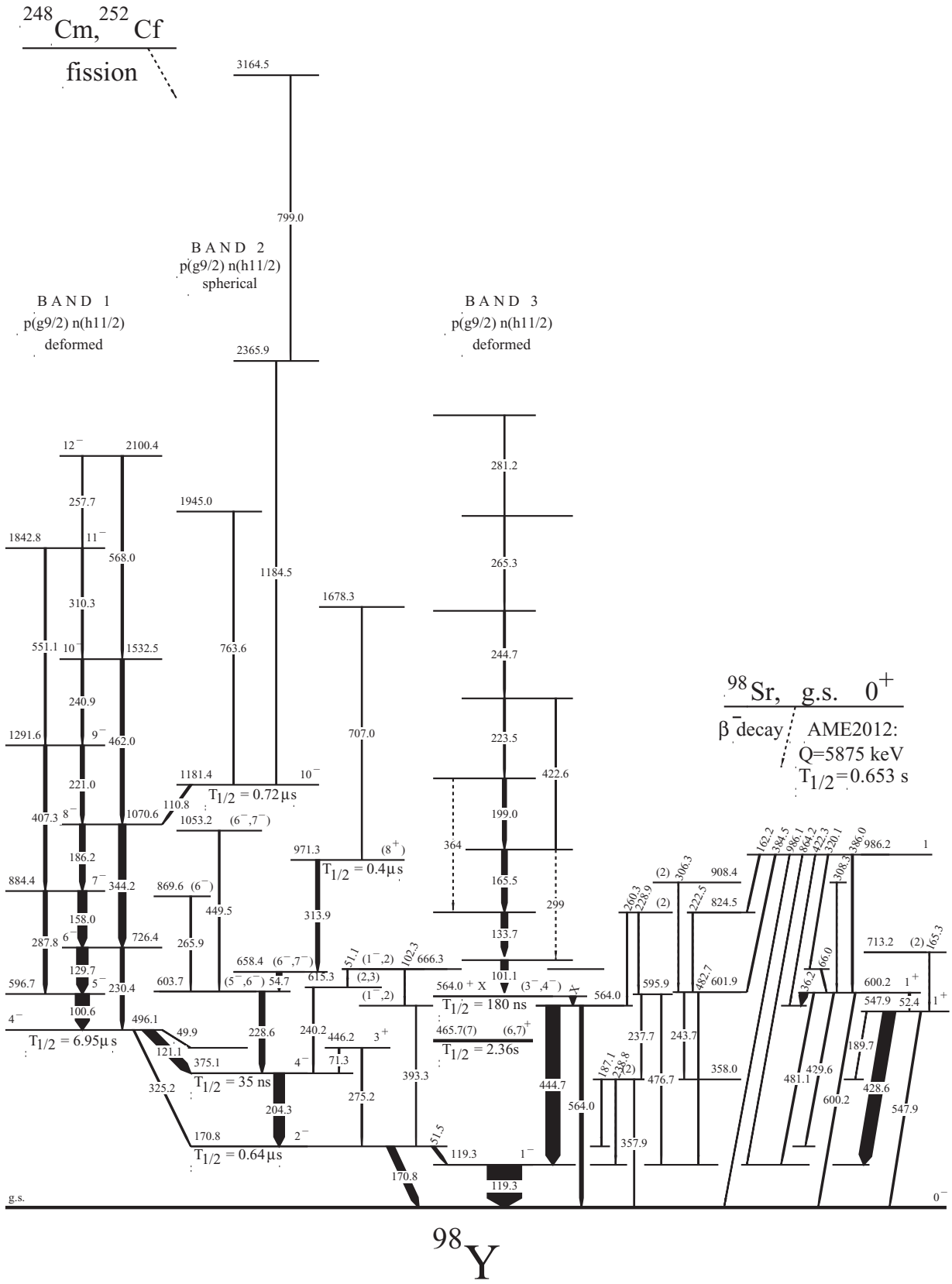

FIG. 2. Partial level scheme of ^{98}Y, as obtained in the present work (AME2012: [35]). See Tables I–VI for more information.

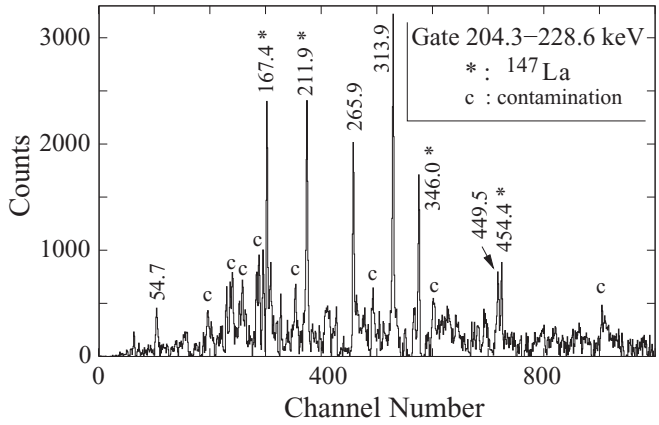

FIG. 3. A γ spectrum doubly gated on the 204.3- and 228.6-keV lines in the ^{248}Cm fission data (Exp. 1).

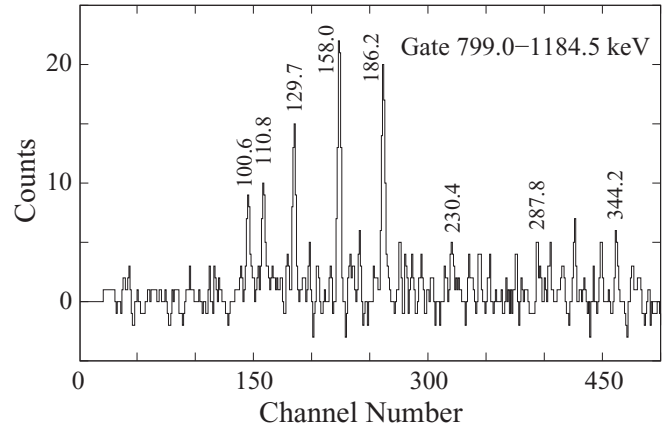

FIG. 5. A delayed γ spectrum doubly gated on the 799.0- and 1184.5-keV prompt γ lines in the *ppd* histogram from the ^{252}Cf fission data.

seen in ^{95}Y [38], ^{96}Y [39,40], or ^{97}Y [41]. Considering that ^{98}Y is at the maximum of the population in fission of yttrium isotopes, one might expect spherical configurations in this nucleus extending up to 4 MeV.

For the ^{252}Cf fission data, (Exp.2), we created *ddp* and *ppd* histograms, used to search for coincidences across isomers. The prompt-γ rays registered from -10 to $+10$ ns relative to the "0" time given by the Mmaster-gate signal were sorted along the p axis. On the d axis we sorted γ rays registered from 40 to 210 ns after the "0" time. Using the *ddp* and *ppd* histograms, we have searched for excitations above the 1181.4- and 971.3-keV isomers. Above the 1181.4-keV isomer we found three transitions of 763.6(3), 799.0(3), and 1184.5(2) keV, as shown in Fig. 2. Figure 5 shows a delayed γ spectrum, doubly gated in the *ppd* histogram on the 799.0- and 1184.5-keV transitions above the 1181.4-keV isomer. In the spectrum all lines in the cascade depopulating the isomer are seen. An analogous search has revealed a prompt γ transition of 707.0(3) keV above the 971.3-keV isomer. Intensities of these transitions are rather low. Relative to the 110.8-keV isomeric transition, with intensity $I_\gamma = 1.00$ in arbitrary units, $I_\gamma(763.6) = 0.07(2)$, $I_\gamma(799.0) = 0.02(1)$, and $I_\gamma(1184.5) = 0.05(2)$. The relative intensity of the 707.0-keV transition is $I_\gamma(707.0) = 0.03(1)$ compared to $I_\gamma(313.9) = 1.00$.

In Fig. 1 there are new lines at 133.7, 165.5, and 199.0 keV. Figure 6 shows a γ spectrum doubly gated on the 133.7-keV line and the 167.4-keV line of ^{147}La. In the spectrum there are prompt-γ lines of ^{147}La, the 165.5- and 199.0-keV lines, another new line at 101.1 keV and, interestingly, the known 119.3- and 444.7-keV lines of ^{98}Y. This suggests a new band above the known 564.0-keV level [12]. Low intensity of the 444.7-keV line in Fig. 6 suggests that the band head is an isomer.

In Fig. 7 we show a γ spectrum cut from a 3D histogram, called *ddp*, containing triple-γ coincidences from Exp. 1, where along the p axis we sorted prompt-γ rays while on both d axes we sorted two γ rays delayed with respect to the prompt. The spectrum shows prompt-γ rays, doubly gated on the 119.3- and 444.7-keV delayed lines. Further gating allowed the construction of a new band, shown as band 3 in Fig. 2.

Energies and relative intensities (in arbitrary units) of prompt-γ transitions from bands 1, 2, and 3 of ^{98}Y, populated

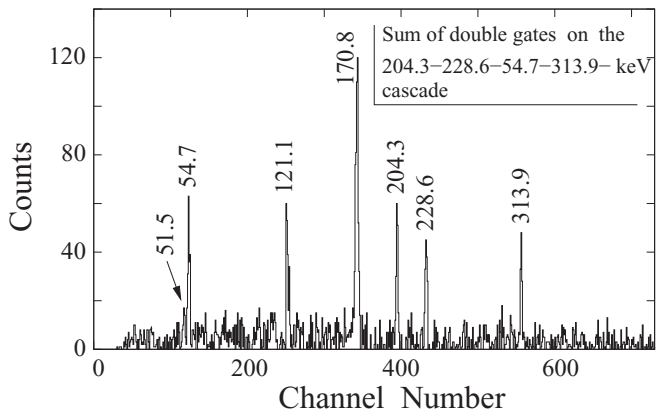

FIG. 4. Sum of γ spectra, double-gated on all pairs of γ lines in the 204.3-228.6-54.7-313.9-keV cascade in ^{98}Y, populated in β^- decay of ^{98}Sr (Exp. 5).

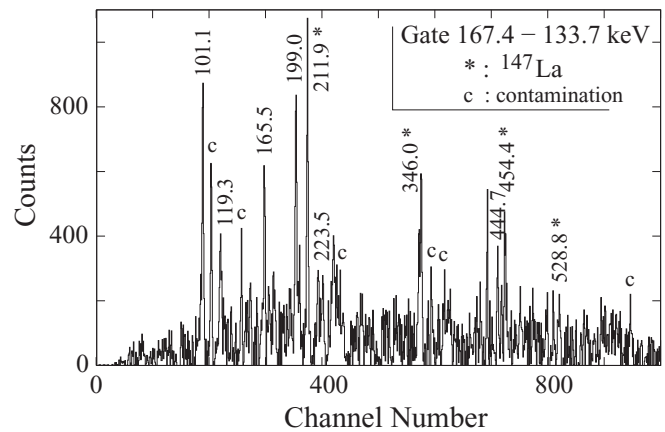

FIG. 6. A γ spectrum doubly gated on the 167.4-keV line of ^{147}La and the 133.7-keV line of ^{98}Y in ^{248}Cm fission data.

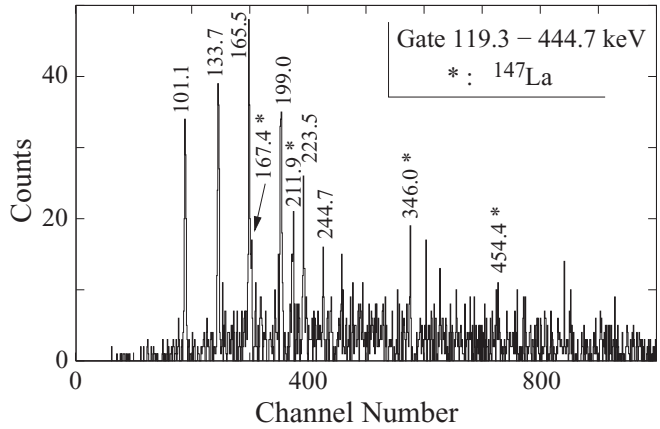

FIG. 7. A γ spectrum doubly gated on the 119.3- and 444.7-keV lines in the *ddp* histogram sorted from ^{248}Cm fission data.

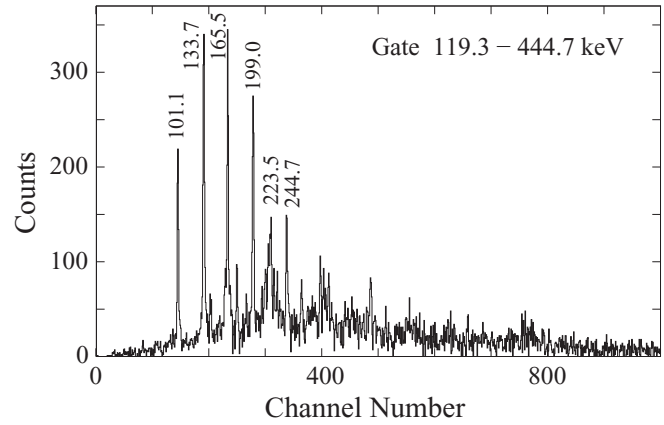

FIG. 8. A γ spectrum doubly gated on the 119.3- and 444.7-keV lines in the *ddp* histogram sorted from the ^{252}Cf fission data.

in spontaneous fission of ^{248}Cm, are shown in Table I. The intensities were obtained from a spectrum doubly gated on the prompt 167.4- and 211.9-keV lines of ^{147}La. In this spectrum the intensities of lines depopulating long-lived isomers at 496.1-, (564.0 + X)- and 1181.4-keV are strongly depressed by the limited time window of Exp. 1 and are not shown in Table I. However, the intensities of prompt lines of the above isomers allow us to compare the populations of bands 1, 2, and 3. It can be seen that the new band 3 is approximately a factor of 3 less intense than the band on top of the 496.1-keV, 4^- isomer.

The new band 3 is confirmed by the ^{252}Cf fission data. Figure 8 shows a spectrum doubly gated on the 119.3- and 444.7-keV lines on the two d axes of the *ddp* histogram. The prompt-γ lines of the new band 3 are clearly seen in the spectrum.

The half-life of the new bandhead, measured using the ^{248}Cm fission data, is 160(40) ns, with large uncertainty due to the limited statistics and short time window of Exp. 1. A better result was obtained from the ^{252}Cf fission data. A *ggt* histogram sorted from this data contains on two g axes energies of two γ rays in a cascade and on the t axis a difference of their time signals. Figure 9 shows a spectrum of time differences, doubly gated on the 444.7-keV line below the isomer and on prompt lines above the (564.0 + X)-keV isomer in ^{98}Y. Fitting the spectrum yields a half-life of $T_{1/2}$ = 180(7) ns for the isomer. The prompt component in Fig. 9 is due to contaminations by prompt lines from other nuclei, unavoidable in such complex data sets. To test the method, we determined the half-life of the known 164.1(9)-ns isomer in ^{134}Te [42], obtaining 165.1(10) ns, and the half-life of the known 375.1-keV, $T_{1/2}$ = 35.8(8) isomer in ^{98}Y [12], obtaining $T_{1/2}$ = 35.0(5) ns (see Table II).

Because the half-life of the 564.0-keV level is known to be 2.4 ns [12], we propose that the isomeric band head of band 3 is located just above the 564.0-keV level.

The isomeric transition, X, shown in Fig. 2, is not observed in the present ^{248}Cm and ^{252}Cf data. However, a possible candidate is seen in the spectrum populated in β^- decay of

TABLE I. Energies and intensities of prompt γ transitions in bands 1, 2, and 3 of ^{98}Y populated in spontaneous fission of ^{248}Cm, as observed in the present work in Exp. 1.

E_γ (keV)	I_γ (rel.)	E_γ (keV)	I_γ (rel.)	E_γ (keV)	I_γ (rel.)
54.7(1)	53(12)	221.0(1)	55(5)	287.8(1)	25(4)
100.6(1)	210(9)	223.5(2)	22(3)	310.3(2)	16(3)
101.1(1)	56(8)	228.6(1)	101(6)	313.9(1)	60(5)
129.7(1)	190(8)	230.4(1)	8(2)	344.2(1)	24(4)
133.7(1)	58(5)	240.9(1)	47(4)	407.3(1)	34(3)
158.0(1)	125(8)	244.7(2)	12(2)	422.6(2)	5(2)
165.5(1)	48(5)	257.7(2)	10(2)	449.5(2)	12(2)
186.2(1)	98(6)	265.3(2)	8(2)	462.0(1)	25(3)
199.0(1)	25(4)	265.9(2)	18(4)	551.1(2)	18(3)
204.3(1)	114(7)	281.2(3)	6(2)	568.0(2)	15(3)

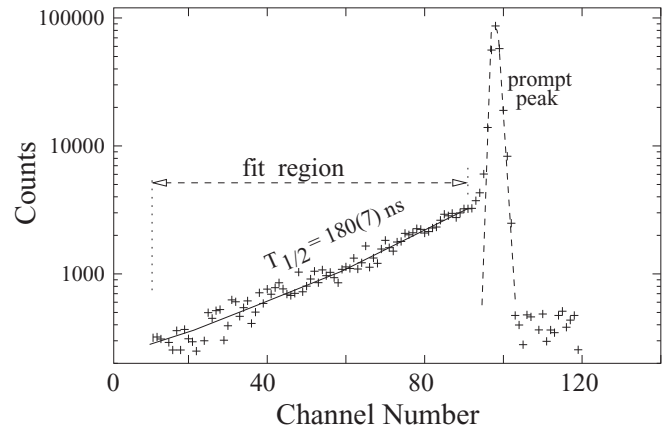

FIG. 9. Time-delayed spectrum corresponding to the decay of the (564.0 + X)-keV isomer in ^{98}Y populated in spontaneous fission of ^{252}Cf, as observed in the present work. The spectrum is gated on the 444.7-keV (gate below the isomer) and the sum of 101.6-, 133.7-, 165.5-, and 199.0-keV lines (gate above the isomer). Time scale is 8.8 ns/channel. The solid line represents the exponent-plus-background fit to the data.

TABLE II. Half-lives of levels in ^{98}Y and ^{98}Sr, as measured in the present work in Exp. 2, Exp. 4, and Exp. 5, in comparison to literature values. See text for further information.

E_{exc} (keV)	$T_{1/2}$ present work	$T_{1/2}$ Ref. [12,43]
	^{98}Y	
170.8(1)	0.64(2) μs	0.610(9) μs
375.1(2)	35.0(5) ns	35.8(8) ns
465.7(7)	2.36(6) s	2.0(2) s
496.1(2)	6.95(6) μs	6.87(5) μs
564.0 + X	180(7) ns	
971.3(4)	0.45(15) μs	
1181.4(5)	0.72(2) μs	0.806(21) μs
	^{98}Sr	
0.0	0.651(2) s	0. 653(2) s

^{98}Sr. In Fig. 10 we show a γ spectrum from Exp. 5, gated on the 444.7-keV line in a $\gamma\gamma$ histogram, sorted in a 600 ns time window. In the spectrum, which contains known lines feeding the 564.0-keV level [12], there is a new line at 26.3 keV. A spectrum gated on this line shows lines at 119.3, 444.7, and 564.0 keV. One is tempted to propose that the 26.3-keV line is from a new, 180-ns isomer to the 564.0-keV level. A stretched $E2$, 26.3-keV decay of the isomer with spin-parity $I = 3^-$ could account for its half-life. However, for the isomer to be visibly populated in β^- decay of the 0^+ ground state of ^{98}Sr, its spin should be lower than $I = 3$ and then the isomeric transition could no longer be a stretched $E2$. The 26.3-keV line, when depopulating the isomer, should show a half-life of 180 ns. However, such low-energy signals in our measuremet show a large "time-jitter" of about 300 ns, disabling meaningful conclusions.

It should be further mentioned that the 26.3 keV line may be due to an effect on the surface of the Ge-detector crystal. After scattering of the 36.2-keV γ photon on the K electron, the X_K radiation escapes the crystal (K binding energy in Ge is about 10 keV), leaving in the crystal the remaining energy. A dedicated experiment is needed to solve the problem of the 26.3 keV line.

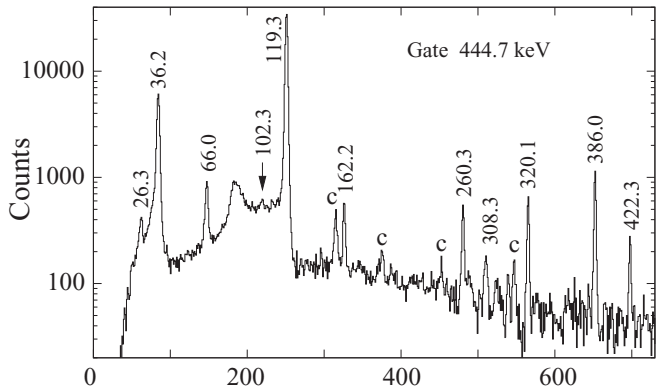

FIG. 10. γ spectrum gated on the 444.7-keV line of ^{98}Y, populated in β^- decay of ^{98}Sr. Label "c" denotes contaminating lines.

TABLE III. Normalized, experimental angular-correlation coefficients, a_k/a_0, and the corresponding mixing ratios, δ, for γ transitions in ^{98}Y, populated in spontaneous fission of ^{252}Cf, determined for various spin hypotheses. The superscript d denotes the transition for which the δ value was deduced. The 428.6- and 36.2-keV transitions are assumed to be pure $E1$ with $\delta = 0$.

Cascade γ_1–γ_2	a_2/a_0 (exp.)	a_4/a_0 (exp.)	Spins I_1, I_2, I_3	$\delta(\gamma)$
36.2–444.7^d	0.09(5)	−0.15(9)	1 → 1 → 1	−0.04(6)
			1 → 2 → 1	0.2(2)
428.6–119.3^d	−0.16(2)	0.07(3)	1 → 1 → 0	0.0(2)
444.7^d–119.3	−0.19(2)	−0.02(3)	1 → 1 → 0	0.04(2)
			2 → 1 → 0	0.4(2)
121.1^d–204.3	0.22(2)	0.09(4)	4 → 4 → 2	−0.8(2)
228.6^d–204.3	0.11(2)	−0.01(4)	5 → 4 → 2	0.31(5)
			5 → 4 → 2	2.5(3)
			6 → 4 → 2	0.0

For a few strong γ-γ cascades in ^{98}Y it was possible to determine angular correlations, which are listed in Table III, where we also show possible solutions for spins in these cascades. The results will be discussed further in Sec. IV.

2. *Study of isomers in the micro- to millisecond range*

From the data of Exp. 4 a gt histogram was sorted with γ energy on the g axis and its time of registration, counted from the start of the deflector cycle, on the t axis. Figure 11 shows the low-energy part of the γ spectrum gated on the "beam ON" range of the time axis, where we subtracted background spectrum gated on the "beam OFF" range. In the spectrum one can see lines corresponding to decays of known isomers at 170.8, 496.1 and 1181.4 keV [12]. There is no 444.7-keV line from the 180-ns isomer, because it decays in the first 1.7 μs after the production, when the ^{98}Y ions fly to the collection point of Lohengrin.

In Fig. 12 we show a γ spectrum obtained in a 1mus time window, counted from the arrival of an ion. The short time window favors microsecond isomers, and the cascade

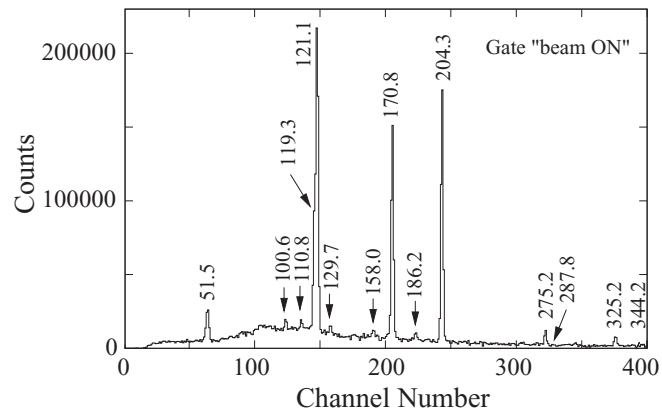

FIG. 11. Low-energy part of the spectrum γ rays from ^{98}Y produced in neutron-induced fission of ^{235}U in Exp. 4, observed in a time window up to 6 ms after the production.

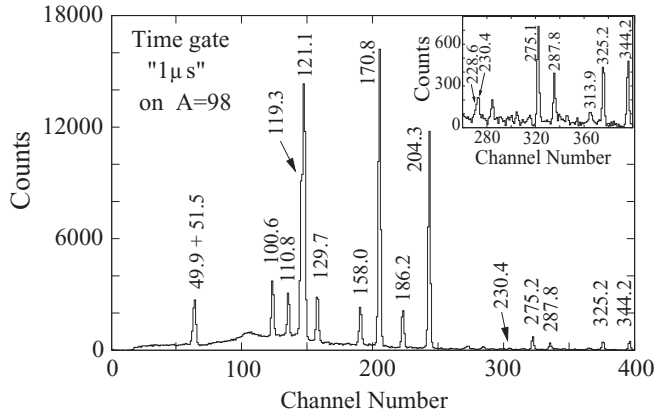

FIG. 12. Low-energy part of the spectrum of γ rays of ^{98}Y populated in neutron-induced fission of ^{235}U in Exp. 4, observed in a 1 μs time window, counted from the arrival of an $A = 98$ ion at the detection point of Lohengrin.

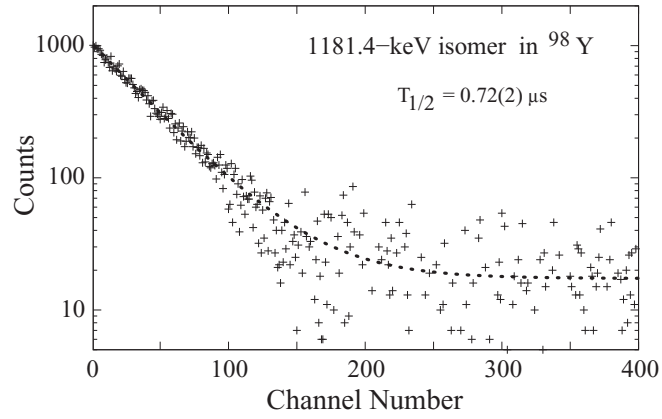

FIG. 13. Time-delayed spectrum corresponding to the summed intensities of the 100.6-, 129.7-, 158.0-, 186.2-, and 110.8-keV γ transitions, depopulating the 1181.4 keV isomer in ^{98}Y, as observed in Exp. 4. Time calibration is 25.0 ns per channel. The dashed line represents the exponent-plus-background fit to the data.

depopulating the 1181.4-keV isomer is now enhanced relative to the decay of the 496.1-keV isomer, as compared to Fig. 11. In Fig. 12 we note weak lines at 228.6 and 313.9 keV, seen in the inset, further supporting the isomeric nature of the 971.3-keV level. In Exp. 4 the population of the new, 971.3-keV isomer is of the order of 10^{-3} of the population of the 496.1-keV isomer, as shown in Table IV.

The time-delayed spectrum, obtained from the gt histogram by summing gates on lines in the 228.6-54.7-313.9-keV cascade, allowed the determination of the upper limit of 0.6 μs for the half-life of the new, 971.3-keV isomer. With the lower limit for observing an isomer at Lohengrin of about 0.3 μs, we estimate the half-life of the 971.3-keV isomer to be 0.45(15) μs.

Figure 13 shows a time-delayed spectrum corresponding to the summed gates on the 100.6-, 129.7-, 158.0-, 186.2-, and 110.8-keV γ lines. The half-life of the 1181.4-keV isomer obtained from this spectrum is $T_{1/2} = 0.72(2)$ μs. We have also measured half-lives of the 170.8- and 496.1-keV isomers in ^{98}Y. Figure 14(a) shows a time-delayed spectrum gated on the 204.3-keV line with a single half-life corresponding to the 496.1-keV isomer. Figure 14(b) shows the time-delayed spectrum gated on the 170.8-keV line, where both half-lives

TABLE IV. Energies and relative intensities of γ transitions deexciting levels populated in decays of the 496.1-, 971.3- and 1181.4-keV isomers in ^{98}Y, as observed in this work in Exp. 4. γ intensities are in arbitrary, relative units.

E_{exc} (keV)	E_γ (keV)	I_γ (rel.)	E_{exc} (keV)	E_γ (keV)	I_γ (rel.)
119.3	119.3(1)	1450(50)	603.7	228.6(1)	8(3)
170.8	51.5(1)	580(30)	726.4	129.7(1)	95(8)
	170.8(1)	3400(100)		230.4(1)	12(4)
375.1	204.3(1)	4440(140)	658.4	54.7(2)	4(2)
446.2	71.3(2)	10(4)	884.4	158.0(1)	98(7)
	275.2(1)	350(20)		287.8(1)	18(3)
496.1	49.9(2)	210(30)	971.3	313.9(1)	7(3)
	121.1(1)	4250(140)	1070.6	186.2(1)	113(8)
	325.2(2)	120(40)[a]		344.2(1)	30(5)
596.7	100.6(1)	100(6)	1181.4	110.8(1)	79(6)

[a]The intensity of the 325.2-keV line has been corrected for the summation effect.

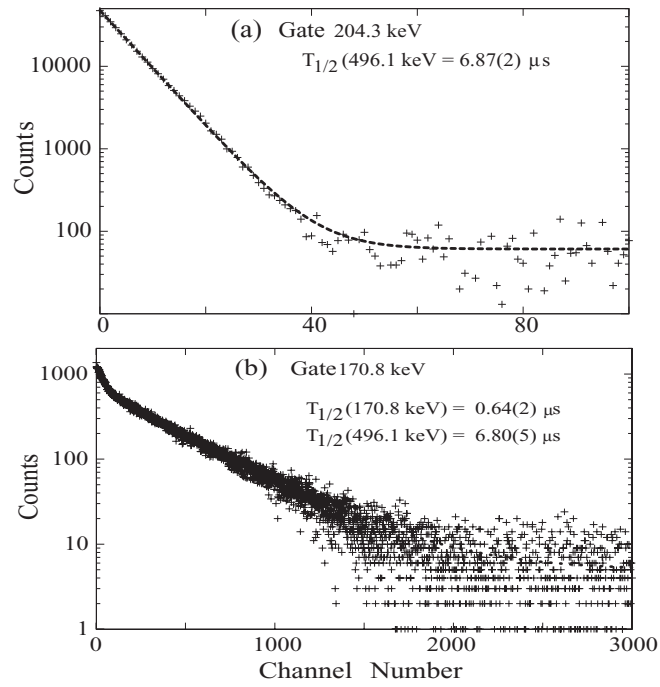

FIG. 14. (a) Time-delayed spectrum gated on the 204.3-keV γ transition, populated by the 496.1-keV isomer in ^{98}Y, as observed in Exp. 4. Time calibration is 1.6 μs per channel. The dashed line represents the exponent-plus-background function fitted to the data. (b) Time-delayed spectrum gated on the 170.8-keV γ transition, populated by the 496.1- and 170.8-keV isomers in ^{98}Y. Time calibration is 25.0 ns per channel. The dashed line represents the two-exponents-plus-background function fitted to the data.

contribute (we neglected in these fits the 35 ns half-life corresponding to the decay of the 375.1-keV level). New half-lives are shown in Table II and compared to the previously measured values [12]. The half-life of the 496.1-keV isomer was increased by 0.10(5) μs, correcting for the beam rate of about 500 ions/s, as discussed in Ref. [38].

The clean data, as shown in Fig. 11, allowed the determination of precise branching ratios for levels populated in the decays of the 170.8-, 496.1-, and 1181.4-keV isomers, which will be analyzed in Sec. IV. The corresponding intensities of γ lines, shown in Table IV, were obtained from a singles spectrum collected within 60 μs after the arrival of an ion. We note a new 325.2-keV branch from the 496.1-keV isomer. The 325.2-keV line, clearly seen in Figs. 11 and 12, shows more intensity than is due to just the summation in our detectors of two strong lines at 121.1 and 204.3 keV. The limit for the summation effect in this measurement is estimated to be 3(1)% of γ intensities in the cascade. The intensity of the 325.2-keV line in Table IV is corrected for the summation effect.

The γ intensities shown in Table IV provide information on conversion coefficients for the low energy transitions involved in the population of isomers in fission, and they allow us to test the consistency of the decay scheme.

The intensity balance for the 446.2-keV level is only consistent with an $E1$ multipolarity for the 49.9-keV transition. The experimental, total conversion coefficient deduced from the balance is 0.73(25). The total feeding of the 170.8-keV level amounts to 5400(150) relative units, taking the corresponding theoretical total conversion coefficients [44] for the 204.3- and 325.2-keV $E2$ transitions and the 275.2-keV $E1$ transition. This number, compared against the total decay intensity (assuming $E2$ multipolarity of the 170.8-keV transition), provides the total conversion coefficient of 1.6(4) for the 51.5-keV transition, indicating its $M1 + E2$ multipolarity. Analogously, intensity balances for the 119.3- and 375.1-keV levels provide the experimental, total conversion coefficients of 0.03(5) and 0.13(5) for the 119.3- and 121.1-keV transitions, respectively.

The total feeding of the 1070.6-keV level is estimated to be 152(10), taking the total conversion coefficient of 0.07(3) for the 186.2-keV transition, where the uncertainty covers the whole range of theoretical values for an $M1 + E2$ multipolarity. This allows us to estimate the total conversion coefficient for the 110.8-keV isomeric transition to be 0.9(2), which indicates its $E2$ character.

From the above we calculated feeding of the 496.1-keV isomer to be 5270(160) relative units. Thus, feeding of the 1181.4-keV isomer is about 0.03 of that of the 496.1-keV isomer, when measured at the focal point of Lohengrin, about 1.7 μs after the production of both isomers in the ^{235}U target.

The total decay intensity from the 496.1-keV isomer, calculated taking γ intensities of the 49.9-, 121.1-, and 325.2-keV transitions and their conversion coefficients, yields 5415(160) relative units, which is consistent with the total feeding of the 170.8-keV level. This is also consistent with the total feeding of the ground state of 5450(150) relative units, obtained taking γ intensities of the 119.3- and 170.8-keV transitions and the total conversion coefficient of 0.06(3) for the 119.3-keV transition from Table VI (see the next section).

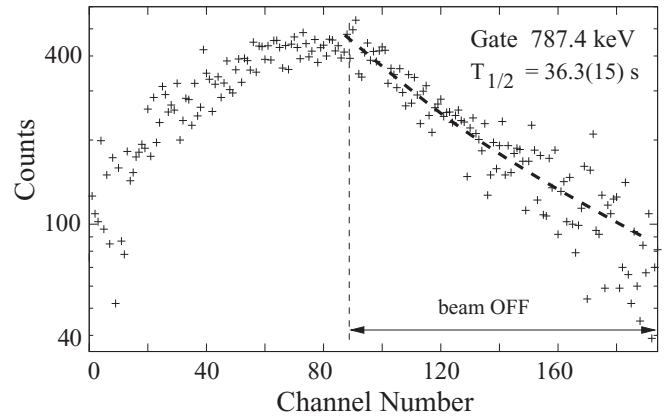

FIG. 15. Time-delayed spectrum gated on the 787.4-keV γ line of ^{98}Mo, obtained in Exp. 3. Time calibration is 1.0245 s/channel. The dashed line represents the exponent-plus-background function fitted to the data.

We conclude that the 170.8-keV isomer does not receive any visible direct feeding in fission. The upper limit is 0.01 of the feeding of the 496.1-keV isomer, as seen at the measurement point of Lohengrin.

3. *Search for isomers in the seconds range*

In Exp. 3 we searched for isomers in the seconds range the $A = 98$ mass chain. The sensitivity of the measurement is illustrated in Fig. 15, showing the time-delayed spectrum gated on the 787.4-keV line in ^{98}Mo populated in β^- decay of ^{98}Nb, which is produced in β^- decay of ^{98}Zr. The $T_{1/2} = 36.3(15)$ s half-life, fitted to the spectrum in the "beam OFF" range, results from the 30.7 s half-life of the ground state of ^{98}Zr and other half-lives in the $A = 98$ mass chain.

In this measurement we observed known half-lives in the $A = 98$ isobars but did not find any evidence for new, long-lived isomers in mass $A = 98$ isobars populated in neutron-induced fission of ^{235}U.

4. *Low-spin excited levels of ^{98}Y populated in β^- decay of ^{98}Sr*

We verified low-spin excitations of ^{98}Y, shown in the right-hand side of Fig. 2, in a measurement of γ rays following β^- decay of ^{98}Sr (Exp. 5). Figures 16(a) and 16(b) show total projections of the data on the E_γ and the time axes of a gt matrix, respectively. The matrix served as a convenient tool to assign γ lines to various decays.

Figure 17 shows examples of time spectra, gated on γ lines of ^{98}Y and ^{98}Zr. The spectrum gated on the 119.3-keV line of ^{98}Y, shown in Fig. 17 (a), provides half-life of 0.652(3) s for the ground state of ^{98}Sr, in agreement with the 0.653(2) s half-life reported in the compilation [12]. This indicates that the 119.3-keV level does not receive any visible population from the 2-s isomer at 465.7 keV in ^{98}Y [12].

A visible drop in channel 1000 in Fig. 17(a) is consistent with the fact that part of the population of the 119.3-keV level is due to the decay of the 496.1-keV isomer. Based on the growth-in and decay curves of Fig. 17(a), we estimated that

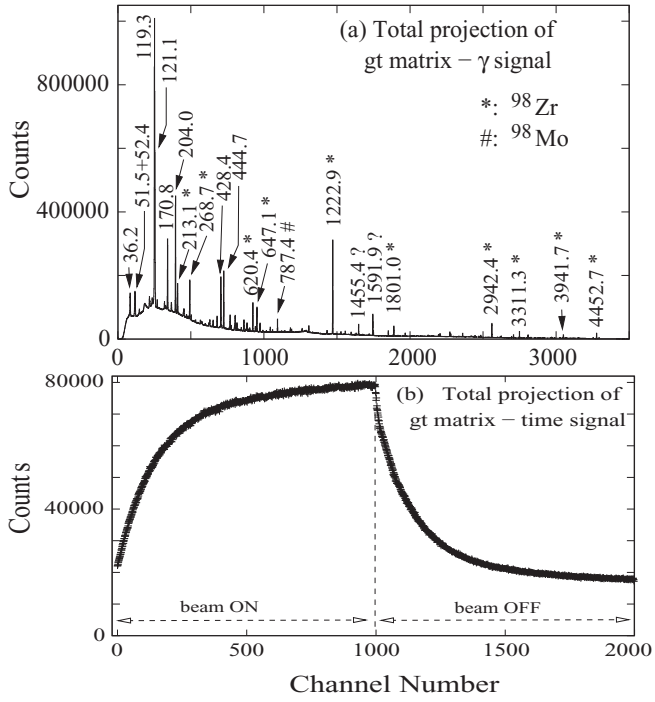

FIG. 16. Total projections on (a) γ-energy axis and (b) time axis of the *gt* matrix obtained in Exp. 5. The constant-peak-width energy calibration in (a) is strongly nonlinear. Time calibration in (b) is 8 ms per channel.

20(2)% of the total intensity of the 119.3-keV line originates from the decay of the 6.95-μs isomer.

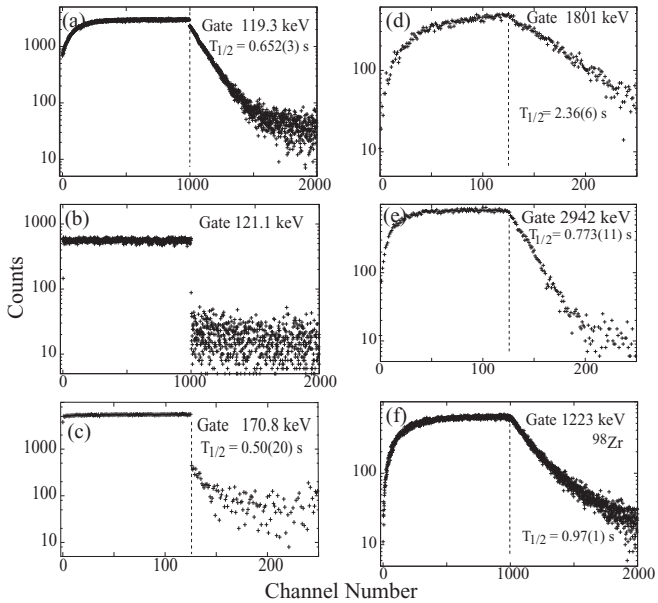

FIG. 17. Time-delayed spectra gated on γ lines of ^{98}Y and ^{98}Zr, obtained in Exp. 5. Time calibration in (a), (b), and (f) is 8 ms per channel. Panels (c), (d), and (e) were binned to 64 ms per channel. Half-lives shown result from fitting a single exponent function plus constant background in the "beam-OFF" ranges. See text for more explanations.

The spectrum gated on the 121.1-keV line of ^{98}Y, shown in Fig. 17(b) [gated on the right-hand part of the (119 + 121)-keV line seen in Fig. 16(a) to avoid contamination from the 119.3-keV line] shows that the 496.1-keV level, depopulated by the 121-keV line, is fed directly in fission only. A similar picture is obtained when gating on the 204.3-keV line. This shows that the 375.1-keV level is populated only in the decay of the 6.95-μs isomer at 496.1 keV, and not via β^- decay of ^{98}Sr or in γ decay of the 2.36-s isomer at 465.7 keV. The upper limit on the population of the 496.1-keV level in β^- decay of ^{98}Sr, estimated from both spectra, is 0.2% of the β^--decay intensity of ^{98}Sr. The same is concluded for the 446.2-keV level based on a spectrum gated on the 275.2-keV line.

In contrast, the spectrum gated on the 170.8-keV line, seen in Fig. 17(c), shows that the 170.8-keV level receives some population in β^- decay of ^{98}Sr. Its amplitude, estimated from the figure, is 12(2)% of the intensity of the 170.8-keV line, seen in Fig. 16(a), which translates to 3.0(6)% of the β^--decay intensity of ^{98}Sr.

We have checked that time spectra gated on lines depopulating the 547.9-, 564.0-, 595.9-, 600.2-, 601.9-, 666.3-, 713.2-, 824.5-, and 986.2-keV levels all are consistent with the half-life of the ground state of ^{98}Sr.

Energies and intensities of γ lines observed in β^- decay of ^{98}Sr in this work are listed in Table V. In the table we included weakly populated levels in ^{98}Y seen above 1 MeV, which are not drawn in Fig. 2 to simplify the picture. The 586.2-keV level and the 603.7- and 752.2-keV transitions reported previously [12] are not confirmed in the present work.

Relative γ intensities from Table V were used to estimate populations of ^{98}Y levels in β^- decay of ^{98}Sr. As a reference we used the sum of known intensities per 100 β^- decays of the two strongest γ lines, $I_\gamma/100(428.6\ \text{keV}) = 27.7(13)$ and $I_\gamma/100(444.7\ \text{keV}) = 33.0(4)$ [12]. Intensities of transitions per 100 decays of the 2.36-s isomer in ^{98}Y were then obtained by multiplying the I_γ values in relative units, shown in Table V by a factor 0.079(3).

The populations, listed in Table V agree with those reported in the compilation [12], except for the population of the 666.3-keV level, which is clearly lower in our data. The high uncertainty on the intensity of the 36.2-keV transition is due to the large uncertainty of the efficiency calibration at this energy, causing large uncertainties of populations of the 564.0- and 600.2-keV levels.

Using these populations, we calculated $\log_{10} ft$ values for levels in ^{98}Y populated in β^- decay of the 0^+ ground (g.s.) state of ^{98}Sr. Our values agree with those reported in Ref. [12]. The only visible difference is for the 666.3-keV level, where we report larger $\log_{10} ft$ value, which does not support the (1^+) spin-parity assignment proposed previously [12]. For the 358.0- and 564.0-keV levels we could propose lower limits for $\log_{10} ft$, only. Spins and parities shown in the first column of Table V are consistent with the present $\log_{10} ft$ values.

The populations of excited levels listed in Table V sum up to 104(9), showing that the population of the ground state of ^{98}Y in β^- decay of ^{98}Sr is low and puts a lower limit of 5.6 on the $\log_{10} ft$ value for the ground state.

Observing intensities of γ lines in various gated spectra, we could estimate total conversion coefficients for some

TABLE V. Properties of levels and their γ decays in ^{98}Y, populated in β^- decay of the 0^+ g.s. of ^{98}Sr, observed in the present work in Exp. 5. See text for more comments.

Level I^π	Level E_{exc} (keV)	γ decay E_γ (keV)	γ decay I_γ (rel.)	Level $P/100$	Level $\log_{10} ft$
0^-	0.0				$\geqslant$5.6
1^-	119.3(1)	119.3(1)	995(38)	12(4)	5.2(2)
2^-	170.8(1)	51.5(1)	10(3)	3.1(8)	5.7(1)
		170.8(1)	52(3)		
(2)	358.0(1)	187.1(2)	20(5)	0.5(7)	$\geqslant$6.4
		238.8(1)	15(3)		
		357.9(2)	2.5(5)		
1^+	547.9(1)	189.7(2)	3.7(5)	24(2)	4.7(1)
		428.6(1)	365(15)		
		547.9(1)	29(1)		
(1^-,2)	564.0(1)	393.3(1)	12(3)	4(8)	$\geqslant$5.0
		444.7(1)	400(15)		
		564.0(1)	89(4)		
(1^-,2)	595.9(1)	237.7(2)	10(5)	1.9(6)	5.8(2)
		476.7(1)	19(1)		
1^+	600.2(1)	36.2(1)	140(30)	43(8)	4.4(1)
		52.4(1)	50(5)		
		429.6(1)	25(4)		
		481.1(1)	100(10)		
		600.2(1)	28(4)		
(1^-,2)	601.9(2)	243.7(2)	10(5)	1.6(6)	5.9(2)
		482.7(2)	10(5)		
(2,3)	615.3(2)	240.2(1)	10(5)	0.0(5)	
(1^-,2)	666.3(1)	51.1(2)	10(5)	1.5(5)	5.9(2)
		66.0(1)	27(2)		
		102.3(1)	2.7(5)		
(2)	713.2(2)	165.3(1)	8.5(5)	0.4(1)	6.4(1)
(2)	824.5(2)	222.5(1)	4(1)	0.7(2)	6.1(1)
		228.9(1)	5(1)		
		260.3(1)	14(1)		
(2)	908.4(2)	306.3(2)	2(1)	0.7(1)	6.1(1)
		308.3(2)	6.4(12)		
1	986.2(1)	162.2(1)	13(2)	7(1)	5.1(1)
		320.1(1)	19(2)		
		384.5(1)	5(2)		
		386.0(1)	39(2)		
		422.3(1)	7.0(5)		
		864.2(2)	2.5(5)		
		986.1(2)	7.0(8)		
(1^-,2)	1199.7(2)	599.3(2)	1.8(5)	1.6(1)	5.6(1)
		651.9(1)	6.1(5)		
		1080.3(2)	12(1)		
(1^-,2)	1348.3(2)	635.6(1)	4.4(5)	0.(7(1)	6.1(1)
		800.3(2)	3.1(6)		
		990.2(2)	1.5(3)		
(1^-,2)	1464.5(3)	798.3(2)	2.4(4)	0.4(1)	6.1(1)
		864.0(2)	2.5(5)		
(1^-,2)	1679.8(4)	1132.4(2)	2.1(6)	0.5(1)	5.6(1)
		1560.5(2)	3.4(5)		
(1^-,2)	1898.6(3)	1298.5(2)	1.8(6)	0.4(1)	5.6(1)
		1334.2(2)	2.7(5)		

TABLE VI. Total conversion coefficients for γ transitions in ^{98}Y, as obtained in the present work, compared to theoretical values [44]. See text for further explanation.

E_γ (keV)	α_{tot}^{exp}	$E1$	α_{tot}^{th} $M1$	$E2$
36.2	1.9(3)	1.99	3.21	40.1
49.9	0.73(25)	0.82	1.31	13.2
51.5	1.2(3)	0.74	1.19	11.7
52.4	2.7(6)	0.70	1.13	10.9
54.7	1.5(3)	0.63	1.01	9.67
66.0	0.3(1)	0.36	0.59	4.84
110.8	0.9(2)	0.08	0.14	0.73
119.3	0.06(4)	0.06	0.11	0.56
121.1	0.13(5)	0.06	0.11	0.53

low-energy transitions in ^{98}Y. The coefficients are listed in Table VI, where we also show theoretical values for pure multipolarities. Some coefficients were derived from the ^{252}Cf fission data and from the intensity balance analysis (the value for the 119.3-keV transition is an average of two values).

B. Excited levels of ^{98}Zr

1. Low-spin level scheme of ^{98}Zr populated in β^- decay of ^{98}Y

Excited levels in ^{98}Zr, populated in β^--decay of the ground state and the 2.36-s isomer of ^{98}Y, have been studied previously in Refs. [45,46], and the data are compiled in Ref. [12]. In the present work we correct and extend these results. The excitation scheme of ^{98}Zr, populated in the β^- decay of both the ground state and the 2.36-s isomer in ^{98}Y is shown in Fig. 18. In Tables VII and VIII we show properties of levels and their γ decays in ^{98}Zr, populated in β^- decay of the ground state and the 2.36-s isomer of ^{98}Y, respectively, as observed in the present work in Exp. 5. In this work we report new levels at 2225.1, 2778.7, 4108.6, 4271.1, 4398.9, and 4492.0 keV but do not confirm the 2047.8-, 2478.9-, 2796.8-, and 3507.0-keV levels and their decays reported earlier [12].

Although in our measurement both β^- decays are observed simultaneously, the very different spins of the ground state and the 2.36-s isomer of ^{98}Y allowed the two decays to be separated. This was further facilitated by observing the half-lives associated with particular γ lines. In Figs. 17(d)–17(f) we show time-decay spectra gated on the 1801.6-, 2942.3-, and 1222.9-keV lines, respectively. The accuracy of time measurements was tested by determining the half-life of the ground state of ^{98}Sr from a spectrum gated on the 428.6- and 444.7-keV lines populated solely in β^- decay of ^{98}Sr (we have checked that the population of ^{98}Rb, which decays to ^{98}Sr, was less than 0.002 of the population of ^{98}Sr in our data). Our half-life of 0.650(5) s compares well with the known value of 0.653(2) s [12].

The half-life $T_{1/2} = 2.36(6)$ s determined from the spectrum gated on the 1801.6-keV line, shown in Fig. 17(d), is consistent with the 2.0(2) s value for the 465.7-keV isomer in ^{98}Y reported in the compilation [12]. As seen in Fig. 17(e), the half-life of the ground state of ^{98}Y is visibly shorter. A "single-decay" fit to the spectrum gated on the 2942-keV line

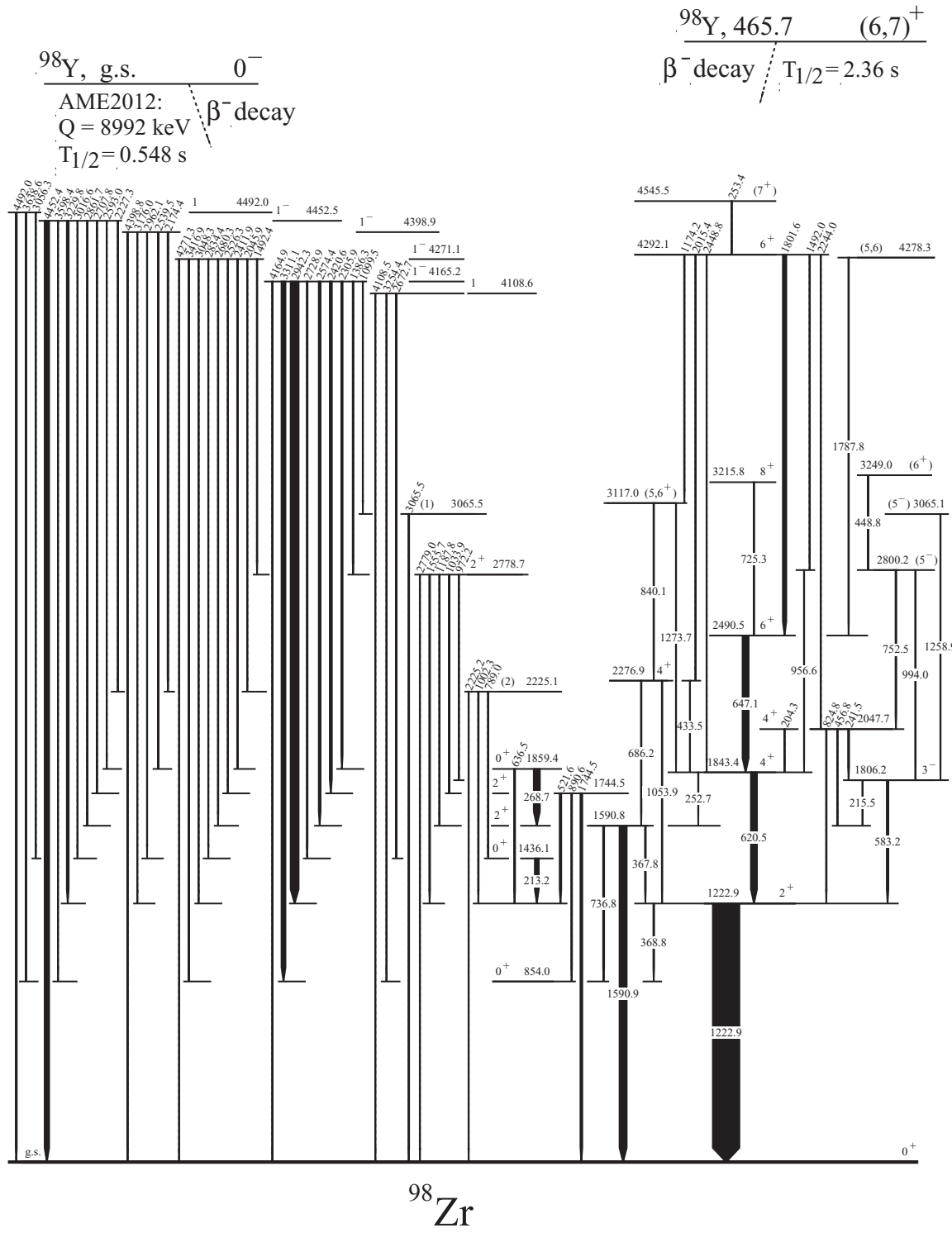

FIG. 18. The ^{98}Zr excitation scheme, as observed in the present work, following β^- decay of the ground state and the 2.36-s isomer of ^{98}Y (Exp. 5), (AME2012: [35]). See the text for more explanations.

provides a value of 0.773(11) s, which combines the 0.653(2) s half-life of the ground states of ^{98}Sr [12]) and the 0.548(2) s half-life of the ground state of ^{98}Y [12]. Finally, the time-decay spectrum gated on the 1222.9-keV line [Fig. 17(f)] is clearly a combination of two decays, of the isomer and the ground state of ^{98}Y.

To determine the population of exited levels in ^{98}Zr in the decay of the ground state of ^{98}Y we took, as the reference, summed intensities of the 2942.3-, 3311.1-, and 4452.4-keV lines, equal to 32.8(22) per 100 decays [12]. Then, the intensities of transitions per 100 decays of the g.s. of ^{98}Y, $I/100$, are obtained by multiplying by a factor 0.054(4) the I_γ

TABLE VII. Levels and their γ decays in ^{98}Zr populated in β^- decay of the g.s. of ^{98}Y, observed in this work in Exp. 5.

Level I^π	Level E_{exc} (keV)	γ-decay E_γ (keV)	γ-decay I_γ (rel.)	Level $P/100$	Level $\log_{10} ft$
0^+	0.0			8(4)	6.1(2)
0^+	854.0(1)			2(2)	$\geqslant$6.2
2^+	1222.9(1)	368.8(1)	25(2)	4.2(15)	8.2(2)[1u]
		1222.9(1)	1000(30)		
0^+	1436.1(1)	213.2(1)	146(5)	6.2(6)	5.9(1)
2^+	1590.8(1)	367.8(1)	31(2)	0.8(4)	8.8(2)[1u]
		736.8(1)	39(2)		
		1590.9(1)	267(8)		
2^+	1744.5(1)	521.6(1)	55(2)	3.1(5)	8.2(1)[1u]
		890.6(1)	30(2)		
		1744.5(1)	70(3)		
0^+	1859.4(1)	268.7(1)	226(7)	11.2(9)	5.5(1)
		636.5(1)	41(2)		
(2)	2225.1(1)	789.0(2)	5(1)	–0.3(3)	
		1002.3(1)	11(2)		
		2225.2(2)	5(2)		
2^+	2778.7(1)	972.2(2)	7(1)	0.0(3)	
		1033.9(3)	5(1)		
		1187.8(2)	4(1)		
		1555.7(1)	28(3)		
		2779.0(2)	4(1)		
(1)	3065.5(2)	3065.5(2	29(2)	1.6(1)	6.0(1)
1	4108.6(2)	2672.7(2)	6(1)	1.1(1)	5.7(1)
		3254.4(2)	10(2)		
		4108.5(2)	4(1)		
1^-	4165.2(1)	1099.5(2)	8(1)	37.9(29)	4.2(1)
		1386.3(1)	32(2)		
		2305.9(1)	48(2)		
		2420.6(1)	76(2)		
		2574.4(1)	66(2)		
		2728.9(1)	22(1)		
		2942.3(1)	288(8)		
		3311.1(1)	151(5)		
		4164.9(2)	11(1)		
1^-	4271.1(1)	1492.4(1)	15(1)	4.2(3	5.1(1)
		2045.9(2)	3(1)		
		2411.9(2)	4(1)		
		2526.3(1)	11(1)		
		2680.3(1)	16(1)		
		2834.4(3)	4(1)		
		3048.3(1)	9(1)		
		3416.9(1)	10(1)		
		4271.3(2)	5(1)		
1^-	4398.9(2)	2174.4(2)	15(5)	3.0(3)	5.2(1)
		2539.5(2)	7(1)		
		2962.1(5)	2(1)		
		3176.0(3)	3(1)		
		4398.8(2)	28(1)		
1^-	4452.5(2)	2227.3(2)	10(2)	14.8(12)	4.5(1)
		2593.0(3)	5(1)		
		2707.8(3)	6(2)		
		2861.7(3)	5(1)		
		3016.6(2)	8(1)		
		3229.8(2)	61(2)		
		3598.4(2)	8(1)		
		4452.4(2)	170(6)		
1	4492.0(2)	3056.3(3)	4(1)	2.4(2)	5.2(1)
		3638.6(3)	4(1)		
		4492.0(2)	36(1)		

values in relative units, shown in Table VII. Using these $I/100$ values we calculated feeding values, $P/100$, for levels in ^{98}Zr, as shown in Table VII. When calculating the populations of 0^+ levels we considered intensities of the $E0$ decays, reported in [12]. The sum of $P/100$ values for exited levels populated in the decay of the g.s. of ^{98}Y is 92(4). Therefore, we propose for the ground state of ^{98}Zr $P/100 = 8(4)$. The obtained $P/100$ values were used to calculate $\log_{10} ft$ values for levels in ^{98}Zr, as shown in the last column of Table VII. To calculate $\log_{10} ft$ values we used the LOG FT program available at [47], taking the half-life of 0.548(2) s and the $Q = 8992(12)$ keV [35] value for the g.s.-to-g.s., β^- decay energy. For levels where the population is zero within the uncertainty, $\log_{10} ft$ values were not calculated.

To calculate populations of exited levels in β^- decay of the 2.36-s isomer of ^{98}Y we took, as a reference, summed intensities of the 1801.6-, 647.1-, and 620.5-keV lines, equal to 143(21) per 100 decays [12]. Then, the intensities of transitions per 100 decays of the 2.36-s isomer in ^{98}Y are obtained by multiplying by a factor 0.245(36) the I_γ values in relative units, shown in Table VIII. Using these $I/100$ values we calculated feeding values, $P/100$, for levels in ^{98}Zr shown in Table VIII. We note that the total of $P/100$ in this decay is 83(10), somewhat below expectation, though the uncertainty of this value may be larger because of a possible systematic error in the normalization factor of 2.1(3) quoted in Ref. [12].

The obtained $P/100$ values were then used to calculate $\log_{10} ft$ values for levels in ^{98}Zr, populated in β^- decay of the 2.36-s isomer in ^{98}Y, as shown in the last column of Table VIII. In the calculation we used the new, 465.7-keV energy of the isomer and its new half-life of 2.36(6) s. Our $P/100$ values and $\log_{10} ft$ values are generally similar to those published earlier [12], though there are some differences which will be discussed in Sec. IV.

2. *Multipolarity measurements for ^{98}Zr*

Results of the angular-correlation analysis for $\gamma\gamma$ cascades in ^{98}Zr, measured in Exp. 2 and Exp. 6, are presented in Table IX, showing experimental a_k/a_0 coefficients and δ mixing ratios derived for various spin hypotheses. The quality of the correlations illustrates the comparison of the experimental a_k/a_0 coefficients to their theoretical counterparts, A_k, [48,49] for cascades of stretched transitions ($\delta = 0$ for both transitions). For the $0 \rightarrow 2 \rightarrow 0$ quadrupole-quadrupole cascade $A_2 = 0.357$ and $A_4 = 1.143$ while for the $4 \rightarrow 2 \rightarrow 0$ cascade $A_2 = 0.102$ and $A_4 = 0.009$. For the stretched dipole-quadrupole cascade, $3 \rightarrow 2 \rightarrow 0$, $A_2 = -0.071$ and

TABLE VIII. Levels and their γ decays in ^{98}Zr populated in β^- decay of the 2.36-s isomer in ^{98}Y, as observed in Exp. 5.

Level I^π	Level E_{exc} (keV)	γ decay E_γ (keV)	γ decay I_γ (rel.)	Level $P/100$	Level $\log_{10} ft$
3^-	1806.2(1)	215.5(2)	4(1)	1.7(18)	
		583.2(1)	60(2)		
4^+	1843.4(1)	252.7(2)	4(1)	−2.9(35)	
		620.5(1)	230(7)		
4^+	2047.7(1)	204.3(1)	5(1)	4(4)	
		241.5(1)	36(3)		
		456.8(2)	4(1)		
		824.8(2)	10(1)		
4^+	2276.9(1)	433.5(1)	5(1)	2(2)	
		686.2(1)	14(1)		
		1053.9(1)	14(1)		
6^+	2490.5(1)	647.1(1)	224(7)	18(4)	5.9(1)
5^-	2800.2(2)	752.5(1)	24(2)	4.2(13)	6.3(2)
		956.6(2)	3(1)		
		994.0(1)	9(2)		
(5^-)	3065.1(3)	1258.9(1)	5(2)	1.2(4)	6.9(2)
$(5,6^+)$	3117.0(2)	840.1(1)	18(2)	2.7(9)	6.5(2)
		1273.7(2)	5(2)		
8^+	3215.8(3)	725.3(2)	4(1)	1.0(3)	7.1(2)
(6^+)	3249.0(3)	448.8(2)	4(1)	1.0(3)	7.1(2)
(5,6)	4278.3(2)	1787.8(1)	15(2)	3.7(8)	6.0(1)
6^+	4292.1(2)	1174.2(2)	12(2)	42(6)	4.9(1)
		1492.0(2)	15(2)		
		1801.6(1)	130(4)		
		2015.4(2)	7(1)		
		2244.0(4)	2(1)		
		2448.8(2)	4(1)		
(7^+)	4545.5(3)	253.4(1)	6(1)	1.5(3)	6.3(1)

$A_4 = 0.00$. We also show the isotropic correlation for the 511.0-keV annihilation peak as seen in the 1222.9-keV gate.

For the 1222.9-, 1436.1-, 1590.8-, 1744.5-, 1806.2-, 1859.4-, and 2047.7-keV levels unique spin-parity assignments are reported in the literature [12]. These assignments agree with the present analysis. For the 620.5-, 647.1-, and 725.3-keV transitions our analysis indicates stretched, quadrupole character. These are then adopted in the "sum" gate (see Table IX).

For strong transitions it was also possible to determine linear polarization of γ transitions by measuring directional-linear-polarization correlations in $\gamma\gamma$ cascades, using the EXOGAM clover detectors of the EXILL array as Compton polarimeters.

The 1222.9-, 620.5-, 647.1-, and 1590.9-keV stretched quadrupole decays in ^{98}Zr [12] served as known, reference transitions for directional-linear-polarization correlations in the measured $\gamma\gamma$ cascades. Results of the linear polarization analysis for γ transitions in ^{98}Zr are shown in Table X in column $P_{exp}(\gamma^p)$.

The last column of Table X shows theoretical values of linear polarization, $P_{th}(\gamma^p)$, which for a mixed dipole-plus-quadrupole transition can be calculated for the upper transition

TABLE IX. Normalized, experimental angular-correlation coefficients, a_k/a_0, and the corresponding mixing ratios, δ, for γ transitions in ^{98}Zr, populated in neutron-induced fission of ^{235}U (Exp. 6) and spontaneous fission of ^{252}Cf (Exp. 2), determined for various spin hypotheses. The 1222.9- and 1590.9-keV transitions are taken as the reference for stretched quadrupole with $\delta(\gamma_2) = 0.0$ [12]. The "sum" denotes summed gates on 1222.9-, 620.5-, and 647.1-keV lines.

Cascade γ_1-γ_2	a_2/a_0 (exp.)	a_4/a_0 (exp.)	Spins I_1, I_2, I_3	$\delta(\gamma_1)$
		^{235}U + n fission		
213.2–1222.9	0.356(23)	1.152(48)	$0 \to 2 \to 0$	
268.7–1590.9	0.340(25)	1.169(48)	$0 \to 2 \to 0$	
511.0–1222.9	0.003(21)	0.017(44)	isotropic	
521.6–1222.9	−0.073(21)	0.016(43)	$2 \to 2 \to 0$	0.44(4)
583.2–1222.9	−0.076(12)	−0.017(27)	$3 \to 2 \to 0$	–0.01(2)
			$2 \to 2 \to 0$	No solution
			$1 \to 2 \to 0$	–0.15(1)
620.5–1222.9	0.102(12)	−0.037(28)	$4 \to 2 \to 0$	
647.1–1222.9	0.105(10)	−0.069(22)	$6 \to 4 \to 2$	
686.2–1590.9	0.13(4)	0.01(8)	$4 \to 2 \to 0$	
824.8–1222.9	0.15(5)	−0.11(12)	$4 \to 2 \to 0$	
1801.6–sum	0.160(16)	0.065(36)	$6 \to 6 \to 4$	–0.77(12)
			$7 \to 6 \to 4$	No solution
2574.4–1590.9	−0.213(28)	0.051(56)	$1 \to 2 \to 0$	–0.03(3)
			$2 \to 2 \to 0$	0.71(8)
			$3 \to 2 \to 0$	–0.18(4)
2680.3–1590.9	−0.28(7)	0.00(13)	$1 \to 2 \to 0$	–0.03(7)
2942.3–1222.9	−0.24(1)	0.01(1)	$0 \to 2 \to 0$	No solution
			$1 \to 2 \to 0$	–0.01(1)
			$2 \to 2 \to 0$	No solution
			$3 \to 2 \to 0$	–0.21(15)
			$4 \to 2 \to 0$	No solution
3229.8–1222.9	−0.29(2)	0.00(5)	$1 \to 2 \to 0$	0.03(2)
			$3 \to 2 \to 0$	–0.29(4)
		^{252}Cf fission		
583.2–1222.9	−0.069(2)	−0.015(18)	$3 \to 2 \to 0$	–0.00(2)
			$2 \to 2 \to 0$	No solution
			$1 \to 2 \to 0$	–0.16(1)
620.5–1222.9	0.095(7)	−0.006(11)	$4 \to 2 \to 0$	
725.3–1222.9	0.089(13)	0.00(2)	$8 \to 6 \to 4$	
1801.6–sum	0.14(2)	−0.04(3)	$6 \to 6 \to 4$	0.17(8)
				–0.80(14)
			$7 \to 6 \to 4$	0.38(6)
				2.3(3)
2942.3–1222.9	−0.25(3)	0.02(4)	$1 \to 2 \to 0$	0.00(3)
			$2 \to 2 \to 0$	No solution
			$0 \to 2 \to 0$	No solution

in a cascade, γ_1, from the formula [27]

$$P_{th}(\gamma_1) = \pm \frac{3A_2B_2 + \frac{5}{4}A_4B_4 + 4A_2(\gamma_2)\frac{2\delta_1 F_2(12I_0I_1)}{1+\delta_1{}^2}}{2 - A_2B_2 + \frac{3}{4}A_4B_4}. \quad (1)$$

In the formula (1) the "+" ("−") sign applies to the $M1 + E2$ ($E1 + M2$) multipolarity of the γ_1 transition (γ^p in Table X). Therefore, comparing the signs of the calculated and the experimental polarizations, one can distinguish between

TABLE X. Experimental, $P_{exp}(\gamma^p)$, and calculated, $P_{th}(\gamma^p)$, values of linear polarization for γ^p transitions in ^{98}Zr, as obtained in the present work. "sum" denotes summed gates on the stretched quadrupole transitions in cascade below the 1801.6-keV transition. See text for further explanation.

Cascade $\gamma_1 \rightarrow \gamma_2$	$P_{exp}(\gamma^p)$	Spins in cascade	Multipolarity of γ^p	δ of γ^p	$P_{th}(\gamma^p)$
1801.6^p–sum	+0.4(15)	$6 \rightarrow 6 \rightarrow 4$	$M1+E2$	−0.78(9)	+0.09(2)
			$M1+E2$	+0.17(8)	+0.29(1)
		$7 \rightarrow 6 \rightarrow 4$	$M1+E2$	+0.38(6)	−0.24(2)
			$M1+E2$	+2.3(3)	−0.32(1)
2942.3^p–1222.9	+0.2(1)	$1 \rightarrow 2 \rightarrow 0$	$E1$	−0.01(1)	+0.34(2)
3229.8^p–1222.9	+0.5(2)	$1 \rightarrow 2 \rightarrow 0$	$E1$	+0.03(2)	+0.32(2)
		$3 \rightarrow 2 \rightarrow 0$	$E1$	−0.29(4)	+0.02(1)

the $M1+E2$ and $E1+M2$ multipolarity of this transition. The A_k, B_k and F_2, coefficients are defined in Refs. [48,49].

The polarization indicates spin-parity 6^+ for the 4292.1-keV level. The solution with $\delta = +0.17(8)$ is preferred. Analogously, spin-parity 1^- is indicated for the 4165.2- and 4452.5-keV levels.

C. Properties of the 2.36-s isomer in ^{98}Y

A $T_{1/2} = 2.0(2)$ s isomer at 410(30) keV in ^{98}Y, with a tentative spin 4 or 5 and unknown parity, was reported in the compilation [29]. Given the 4^- spin-parity, assignment to the 375.1-keV level [12] the (4,5) spin assignment seems unlikely, unless the excitation energy of the isomer is lower than 375.1 keV. Recent evaluation [43] reports this isomer at 241(29) keV, clearly off the previous value, considering the quoted uncertainties. We note that this large change was due to a new measurement of the ground-state mass of ^{98}Y [50]. It is obvious that a precise measurement of the excitation energy for the isomer is needed.

In the experiment at the JYFLTRAP Penning trap, performed in this work (Exp. 7), the measured frequency ratio for the $^{98}Y^{g.s.}$ singly charged ions, relative to $^{98}Y^m$, is $\nu_c^{g.s.}/\nu_c^m = 1.000\,005\,106(8)$. Taking the mass excess of −72 295(8) keV/c^2 for ^{98}Y [43] and the atomic mass unit of 931 494.003 8(4) keV/c^2, one obtains the excitation energy of 2.36-s isomeric state of 465.7(7) keV.

Considering the new, precise excitation energy and the absence of any γ decay of the 2.36-s isomer to either the 375.1- or 170.8-keV levels, one can reject spin and parity (4,5) for this isomer (the upper limit for the unobserved, 90.6-keV decay to the 4^-, 375.1-keV level is about 10^{-4} of the intensity of the 121.1-keV transition). A spin and parity hypothesis of 6^- is also unlikely, due to the same reason. The upper limit of $I = 7$ for the spin and positive parity is set by the observed β-decay properties of this isomer, as will be discussed in the next section. This leaves a spin 6^+ or 7^+ assignment to the 2.36-s isomer in ^{98}Y.

Using the prompt-γ data from fission of ^{248}Cm, we have searched for a deformed band on top of the 2.36-s isomer in ^{98}Y, reported as the most deformed state of all yttrium isotopes [9]. Because of the high spin of the isomer [12], the band should be yrast and populated in fission. Figure 19 shows the low-energy part of a γ spectrum doubly gated on the 167.4- and 211.9-keV lines of ^{147}La, the strongest fission fragment complementary to ^{98}Y in fission of ^{248}Cm. Clearly seen in the spectrum are lines corresponding to the known deformed bands in ^{98}Y and ^{99}Y. With the first gate on the 167.4-keV line, we have set the second gate on all lines seen in this spectrum, one by one, up to 3 MeV. Example spectra (Figs. 1 and 6) show that this method is quite sensitive. Despite that, we did not identify any deformed band or any irregular cascade populating the 2.36-s isomer in ^{98}Y. The upper limit on the intensity of such an unobserved band is about 5% of the intensity of the band on top of the 496.1-keV, 4^- isomer in ^{98}Y. The negative result suggests that the spin of the isomer is higher than the presently adopted value of $I = (4,5)$ [12], considering that the maximum population of yrast levels in fission is around spin $I = 7$ [51].

The difficult-to-observe Y-Pr prompt cross-coincidences have disabled searching for a possible cascade on top of the 2.36-s isomer in the ^{252}Cf fission data.

Relative intensities, I_γ, shown in Tables V, VII, and VIII are given in the same relative units, because they were obtained from the same singles spectrum shown in Fig. 16(a), accumulated over the 8 s "beam ON" and 8 s "beam OFF." Exceptionally, the intensities of the 51.5-, 119.3-, and 170.8-keV lines were determined, relative to the 444.7-keV line, from the "beam-OFF" range only, to exclude the population of these lines in the decay of the 6.95 μs isomer, present in the "beam ON" range.

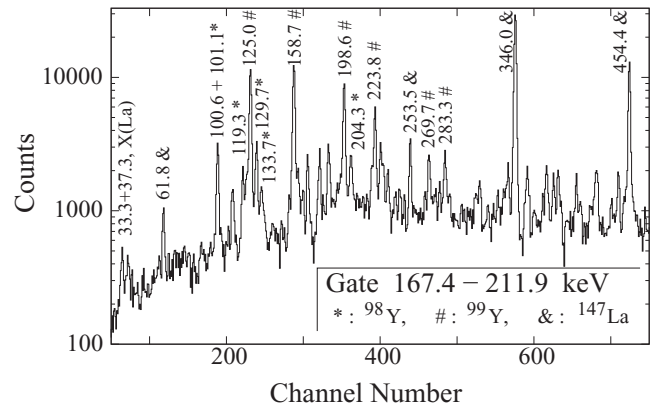

FIG. 19. A γ spectrum doubly gated on the 167.4- and 211.9-keV lines of ^{147}La in the ^{248}Cm fission data (Exp. 1).

Using these I_γ values we can estimate the relative, direct population in fission of ^{235}U induced by thermal neutrons of ground states of ^{98}Sr and ^{98}Y and the 2.36-s isomer in ^{98}Y. We assume that the 8 + 8 s interval of data collection is sufficient to obtain the equilibrium for β^- decays of ground states of ^{98}Sr and ^{98}Y. However, the longer half-life of the 2.36-s isomer results in only 80% saturation.

The relative populations obtained are 0.81(3), 0.38(9), and 0.33(7) for the direct population in fission of the g.s. of ^{98}Sr, g.s of ^{98}Y, and the 2.36-s isomer in ^{98}Y, respectively. When calculating the population of the g.s. of ^{98}Y we subtracted the contribution from β^- decay of the g.s. of ^{98}Sr at the collection point. Further corrections may be required, because our ratios are determined from a single mass-charge-energy setting of the Lohengrin separator.

IV. DISCUSSION

Spins and parity assignments to the ground state and the microsecond isomers at 496.1 and 1181.4 keV in ^{98}Y have changed in the past, involving essential reassignments of proton-neutron configurations to these levels [8,22,36,52]. We note that the most recent spin assignments are still tentative [12]. Furthermore, the 2.36-s isomer in ^{98}Y, reported to have the highest deformation of all yttrium isotopes [9], is a rather mysterious state, considering its "impossible" spin assignment reported in Ref. [12]. In the following we will review the existing information and add our results to get a more reliable picture of this nucleus. We will also review the properties of β^- decays of ^{98}Y and the levels populated in ^{98}Zr.

A. Configurations in ^{98}Y

1. The ground state

The ground state in ^{98}Y was first assigned positive parity to account for the 65% population in β^- decay of the 0^+ g.s. of ^{98}Sr reported in [53]. Absolute intensities of decays to excited states in ^{98}Y, reported later [22], are about a factor 4 higher, implying small feeding to the ground state of ^{98}Y and allowing a negative parity assignment. The negative parity was then proposed [22] based on the well established 1^+ spin-parity of the 600.2-keV level, populated with $\log_{10} ft = 4.3$, and on the measured $E1$ multipolarity of the 36.2-keV transition and $M1 + E2$ multipolarities of the 119.3- and 444.7-keV transitions [53].

Spin $I = 1$ of the ground state, reported in [22], was based on two arguments: (i) that there is a substantial feeding of the 2_1^+ level in ^{98}Zr in β^- decay of the ^{98}Y ground state and (ii) that the 0^- configuration is not expected in ^{98}Y [22]. On that latter issue the authors contradicted themselves, quoting the 0^- assignment for the ground state of the odd-odd neighbor ^{96}Y as an example. An unpublished study [23], compiled in [12], quotes spin-parity $(0)^-$, though it does not present any experimental arguments. Finally, the most recent work [52] repeats the 0^- assignment, though based on calculations only, suggesting the $(\pi p_{1/2} \nu s_{1/2})_{0^-}$, spherical configuration for the ground state of ^{98}Y.

Our data are consistent with the 0^- spin-parity assignment for the ground state of ^{98}Y. The population of 8.1(17)% of all 2^+ levels in ^{98}Zr in β^- decay of the ^{98}Y ground state is nearly a factor 4 lower than the population of 30.1(46)% of all 0^+ levels, as found in the present work. This favors the 0^- spin assignment to the ground state (the present feeding of 2^+ levels in ^{98}Zr is about factor 2 lower than reported previously [12]). The $\log_{10} ft \geqslant 5.5$ to the g.s. of ^{98}Y excludes spin-parity 0^+ for this level.

2. The 547.9-, 600.2-, and 666.3-keV levels

We confirm the 1^+ spin-parity assignment of the 600.2-keV level [22,52]. A $\log_{10} ft = 4.4$ value to this level was determined in the present work for the β^- decay of the 0^+ ground state of ^{98}Sr. The decay is likely the Gamow-Teller (G-T) transition between the $g_{7/2}$ neutron and the $g_{9/2}$ proton orbitals. A similar conclusion is drawn for the 547.9-keV level with $\log_{10} ft = 4.7$, confirming its 1^+ spin-parity assignment [12].

Both levels are composed of the $g_{9/2}$ proton and the $g_{7/2}$ neutron orbitals, but, as proposed in Ref. [52], the 600.2-keV level corresponds to the $(\pi 5/2^+[422], \nu 3/2^+[422])_{1^+}$ deformed configuration, while the 547.9-keV level corresponds to the $(\pi g_{9/2}, \nu g_{7/2})_{1^+}$ spherical configuration. This would represent yet another pair of levels, with the same proton and neutron coexisting in both a spherical and a deformed state. However, we could not confirm the proposition of Ref. [52] that the 600.2-keV level is strongly deformed. While there may be a still undiscovered deformed band on top of this level, the 666.3-keV level is not a member of this band, as proposed earlier [52]. The spin of the 666.3-keV level is probably 2 but we could not identify any other level decaying to the 666.3-keV level. We also note that the 666.3-keV level decays to two other levels, an unlikely feature of an in-band excitation.

3. The 119.3- and 564.0-keV levels

The conversion coefficient of 1.9(3) obtained in this work for the 36.2-keV transition indicates its $E1$ multipolarity and, thus, negative parity for the 564.0-keV level. Angular correlations for the 36.2-444.7-keV cascade, shown in Table III (with $\delta = 0$ of the 36.2-keV transition) allow spin 1 or 2 for the 564.0-keV level.

For the 119.3-keV level spin $I = 2$ was proposed [22], based on small feeding from the ground-state β^- decay of ^{98}Sr. Feeding of the 119.3-keV level seen in this work is significant ($\log_{10} ft = 5.2$), supporting spin-parity 1^- for this level [12], rather than 2^- proposed in Ref. [22]. Angular correlations for the 119.3-428.6-keV cascade also suggest spin 1 for the 119.3-keV level.

The hindrance of the 51.5-keV transition of 2.9×10^4 is high as for an $M1 + E2$ transition (the hindrance for the 170.8-keV, $E2$ transition is 6.9 and the hindrance of the 119.3-keV, $M1 + E2$ transition is 10.5). We also note that the conversion coefficient for the 119.3-keV transition is consistent with either $E1$ or pure $M1$ multipolarity. Thus, positive parity could be considered for the 119.3-keV level. Low-energy 1^+ deformed levels with rotational bands on top of them are known in ^{100,102}Y and ^{102,104}Nb [36,54]. However, we did not find any deformed band on top of the 119.3-keV level. Furthermore, with spin-parity 1^+, the 119.3-keV level should

receive higher population in β^- decay. Therefore, we assign negative parity to this level. The negative parity is supported by the conversion coefficient of the 51.5-keV transition, if the spin and parity of the 170.8-keV level is 2^-, as discussed below.

4. The 496.1-keV isomer and band 1

A tentative (2^-) spin-parity assignment to the 496.1-keV isomer proposed in Refs. [12,22,36,55] has been changed to 4^- in Ref. [52] based on the Interacting Boson Fermion Fermion Model (IBFFM) calculations and in Ref. [8] based on the g factor and the spin-alignment analysis for the band on top of the isomer.

We confirm the recent extension [37] of the band on top of the isomer to spin 12^-. The Quasi-Particle Rotor Model (QPRM) calculations in Ref. [37] well reproduce the band when assuming a $(\pi 5/2^+[422], \nu 3/2^-[541])_{4^-}$ configuration for the 496.1-keV isomer, which was also proposed in Refs. [8,52].

In this work no population of the isomer is observed in β^- decay of ^{98}Sr, indicating, thus, spin higher than 2 for this level. We adopt spin-parity 4^-, after Refs. [8,37,52] but stress that this assignment needs proper, experimental confirmation.

The decays of the isomer are strongly hindered. For the 49.9-keV, $E1$ transition we calculate the rate of 2×10^{-8} W.u. This is about 2–3 orders of magnitude lower than typical low-energy $E1$ rates. For the 121.1-keV transition we obtain a rate of 1.3×10^{-6} W.u. for the $M1$ part and 5×10^{-2} W.u. for the $E2$ component. For the 325.2-keV transition the rate is 2.7×10^{-5} W.u., which is higher than for the $E2$ component of the 121.1-keV transition. Such hindrances could be due to both the K hindrance and differences in shapes of levels in a decay of a deformed level with $K = 4$ to spherical configurations.

5. The 170.8- and 375.1-keV levels and band 2

The 4^- spin-parity of the 496.1-keV isomer and the observation of the 325.2-170.8-keV cascade from the isomer to the 0^- ground state are only consistent with spin-parity 2^- of the 170.8-keV level, considering the half-life of the 170.8-keV level of 0.64 μs. Such spin is not in conflict with the $\log_{10} ft = 5.7$ observed for the 170.8-keV level.

The lack of population in the β^- decay of ^{98}Sr of the 375.1-keV level indicates its spin is higher than 2. Angular correlations for the 121.1-204.3-keV cascade are consistent with spin-parity 4^- for the 375.1-keV level. The δ=0.8 value of the 121.1-keV transition indicates an $M1 + E2$ multipolarity, which is supported by its conversion coefficient.

A prompt-γ study [36] reported the 228.6-, 265.9-, and 313.9-keV transitions in a cascade feeding the 375.1-keV level. We confirm these transitions and add four more transitions to an irregular cascade, shown in Fig. 2. The new 54.7-keV transition is placed between the 228.6- and 313.9-keV transitions.

The relative feeding of the 971.3-keV level seen in the prompt-γ data from fission of ^{248}Cm is much higher than observed in the Lohengrin data, as can be seen in Tables I and IV. Moreover, the 228.6- and 313.9-keV lines are in prompt coincidences with lines of the complementary fission fragment, ^{147}La. This indicates the near-yrast character of the 603.7-, 658.4-, and 971.3-keV levels; therefore, their spins grow with the excitation energy in the cascade.

Angular correlations for the 204.3-228.6-keV cascade (together with the deduced δ values) are consistent with spin-parity 5^- or 6^- for the 603.7-keV level. As the multipolarities of the 228.6- and 54.7-keV transitions are $M1 + E2$ or $E2$ and $M1 + E2$, respectively, negative parity and spins as shown in Fig. 2 are proposed for the 603.7- and 658.4-keV levels. Spin $I = 6$ of the 603.7-keV level is less likely because then, being very yrast, this level should receive higher population in fission. Similar arguments suggest spins for the 869.6- and 1053.2-keV levels, as shown in Fig. 2.

Spherical configurations in ^{98}Y were first reported in Ref. [22] as resulting from coupling of valence neutrons and a proton hole outside the spherical ^{98}Zr core, producing the spherical ground state and the 119.3-, 170.8-, and 375.1-keV levels. Later the 10^-, 1181.4-keV spherical isomer was added to this list [8,52]. Thus a spherical and a well deformed coupling of the $\pi g_{9/2}$ and $\nu h_{11/2}$ unique-parity orbitals are observed in one nucleus. The deformed configuration of the 496.1-keV isomer is convincingly proposed as $(\pi 5/2^+[422], \nu 3/2^-[541])_{4^-}$. Members of the irregular band 2 may belong to the same spherical $(\pi g_{9/2}, \nu h_{11/2})_j$ coupling as the 1181.4-keV spherical isomer. The Generalized Intermediate Coupling Model (GICM) [56] calculations done in Ref. [37] partly reproduce such a band of negative-parity, spherical levels.

6. The 971.3-keV isomer

The spin of the 971.3-keV level should be higher than the spin of the 658.4-keV level but lower than $I = 9$, because of no link with the 1181.4-keV isomer. We propose a spin of $I = 8$ for the 971.3-keV level. Positive parity is proposed tentatively, because of the isomeric nature of the level.

An $I^\pi = 8^+$ spin-parity assignment is attractive, because of the $(\pi g_{9/2}, \nu g_{7/2})_{8^+}$ configuration expected at this excitation energy. Such configuration is observed at 1140 keV in ^{96}Y as an isomer with $T_{1/2} = 9.6$ s [57]. The 8^+ isomer in ^{96}Y has spherical shape, as shown in Ref. [9] and in the recent study [40], where nonrotational cascades are identified on top of the isomer. The observation of the 707.0-keV transition feeding the 971.3-keV isomer in ^{98}Y suggests that it has the same nature as the 8^+ isomer in ^{96}Y.

The IBFFM calculations predicted this level at 1245 keV in ^{96}Y [46,55], after normalizing the $(\pi g_{9/2}, \nu g_{7/2})_{1^+}$ coupling to the experimental 1^+ level at 932 keV. In ^{98}Y the 8^+ is predicted at 977 keV in the IBFFM calculation [46], after normalizing the $(\pi g_{9/2}, \nu g_{7/2})_{1^+}$ coupling to the experimental 1^+ level at 548 keV.

In the context of the rather good reproduction of these experimental data, it is worth mentioning the conclusion of Ref. [55] that the residual interaction between the $g_{9/2}$ protons and the $g_{7/2}$ neutrons does not show any enhancement compared to standard values. This does not support the special role of this particular p-n interaction proposed in the region [58,59] and exploited intensively in recent calculations [10], which suggest that the $\pi g_{9/2}$-$\nu g_{7/2}$ interaction causes large population of the proton $g_{9/2}$ orbital, producing large deformation.

7. The 1181.4-keV isomer

The observation of high-energy transitions feeding the 1181.4-keV isomer in ^{98}Y confirms its spherical shape, proposed in Ref. [52].

8. The 3$^+$, 446.2-keV level

Negative parity assignment to the 446.2-keV level in Ref. [37] was suggested by the GICM calculations and probably by Ref. [52], where a 3^-, level was predicted in the IBFFM calculations as the Gallagher-Moszkowski (G-M) partner to the $(\pi p_{1/2}, \nu g_{7/2})_{4^-}$ configuration proposed for the 375.1-keV level. The negative-parity assignment in Ref. [52] was based on their K-conversion coefficient of the 71-keV transition. In our data this transition is too weak to determine its conversion. We note that the compilation [12] does not report an $M1 + E2$ character of the 71.3-keV transition.

In this work we assign spin-parity 3^+ to the 446.2-keV level, based on the $E1$ multipolarity of the 49.9-keV transition, derived from its total conversion coefficient. The hindrance of 4×10^7 is typical of an $E1$ transition in a spherical nucleus. This assignment agrees with the compilation [12].

We searched for a rotational band on top of the 446.2-keV level with no positive result. It is likely that the 446.2-keV level is spherical. Considering its I^π=3$^+$ spin-parity and the involvement of the $p_{1/2}$ proton and the $h_{11/2}$ neutron, spherical orbitals can be excluded. The $g_{9/2}$ proton coupled to the d or g neutron may produce a spherical 3^+ configuration. The $(\pi g_{9/2}, \nu d_{3/2})_{3^+}$ configuration was indeed predicted at 0.4 MeV by the IBFFM calculations [52].

9. The (564.0 + X)-keV isomer and band 3

The new rotational band on top of the $(564.0 + X)$-keV isomer enhances the picture of the shape coexistence in ^{98}Y, and it is of high interest to identify its structure. The deformed state at $564.0 + X$ keV has spin-parity 3^- or 4^-. In the case where the spin of the 564.0-keV level is 1^-, the spin of the $(564.0 + X)$-keV isomer could be 2 or 3. If the spin of the 564.0-keV level is 2^- the spin of the $(564.0 + X)$-keV isomer could be 4. Spin $I = 2$ for the $(564.0 + X)$-keV isomer is not likely because (i) the $(564.0 + X)$-keV level does not decay to other low-spin levels and (ii) the in-band energies are nearly identical with energies in the $K = 4$ band on top of the 496.1-keV isomer. Considering the observed half-life of the $(564.0 + X)$-keV level, the isomeric transition could have either an $E1$, $M1 + E2$, or stretched $E2$ multipolarity, favoring spins 3^-, 3^+, and 4^- for the isomer.

The 564.0-keV level, to which band 3 deexcites, was proposed to be the $|K_p - K_n| = 1$, G-M partner to the $|K_p + K_n| = 4$ isomer at 496.1 keV [52]. The QPRM calculations performed in this work indeed predict close lying 1^- and 4^- deformed levels, originating from coupling the $5/2^+[422]$ proton orbital with the $3/2^-[541]$ neutron orbital, as shown in Fig. 20. In the figure the calculations are normalized to the experiment at the 496.1-keV isomer, and for the (3^-) isomer we assumed the excitation energy of (564.0+26) keV. The agreement is appealing, though the question remains about the 1^- and 2^- members of the band. One of them may correspond to the 564.0-keV experimental level, if some unknown distortion is assumed at the bottom of the $K = 1$ band.

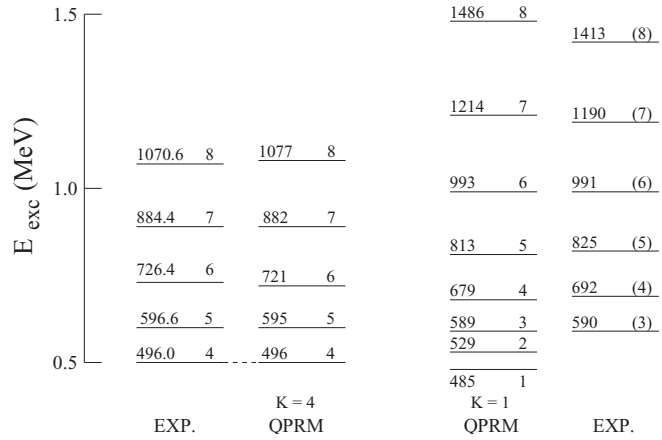

FIG. 20. The QPRM calculations of negative-parity levels in ^{98}Y, based on the $(\pi 5/2^+[422], \nu 3/2^-[541])_{1^-,4^-}$ dominant configurations.

The proposed picture has some disadvantages. The $(M1 + E2)/E2$ branchings for levels in the new band 3 are about an order of magnitude higher than in band 1. This suggests the structure of band 3 is different from the structure of band 1. Furthermore, the 1^- and 2^- of the suggested $K = 1$ band are still not identified. Therefore, one has to consider other possibilities.

In Ref. [52] a 3^- deformed level was predicted just below the 4^-, 496.1-keV deformed isomer. Possible configurations for this level are $(\pi 3/2^-[301], \nu 3/2^+[422])_{3^-}$ or $(\pi 3/2^-[301], \nu 9/2^+[404])_{3^-}$.

There are also more exotic possibilities. First, the IBFFM calculations of Ref. [52] predict 2^+ and 4^+, deformed levels between 500 and 600 keV. Second, in ^{100}Nb, the isotone of ^{98}Y, and in ^{102}Nb, rotational cascades based on deformed 1^+ levels are observed, which show the same characteristic feature of low $E2$ branchings as the band on top of the $(564.0 + X)$-keV isomer. The kinematic moment of inertia for the 1^+ band in ^{102}Nb is identical to that of the $(564.0 + X)$-keV band. When applying this picture to the $(564.0 + 26)$-keV band one should again assume some distortion at the bottom of the band. The eventual link to the, presumably deformed, 1^+ level at 600.2-keV in ^{98}Y remains an open question.

10. The 2.36-s isomer at 465.7 keV

The IBFFM calculations of Ref. [52] predicted the $(\pi g_{9/2}, \nu s_{1/2})_{5^+}$ spherical configuration at 370 keV, which was assigned by the authors to the 2.36-s isomer in ^{98}Y. The very long half-life, and the lack of any decay to the 4^- level at 375.1 keV, were explained as being due to very pure configurations of both levels. This picture is at odds with the result of Ref. [9], which reports high deformation for the 2.36-s isomer in ^{98}Y.

The $I = (4,5)$ spin assignment for the 2.36-s isomer in ^{98}Y was based on the 12% feeding of the 4^+, 1843.4-keV level in ^{98}Zr in β^- decay of the isomer [12]. In the present work this feeding is not observed, while the feeding of the 6^+ level

at 2490.5 keV is increased from 10% to 20% and population of the 8^+ level at 3215.8 keV is observed. We also do not confirm the 3.2% feeding of the 3^- level at 1806.2 keV. In our data it is zero within the uncertainty. The population of the 5^-, 2800.2-keV level is rather low, with a corresponding $\log_{10} ft = 6.3$.

Our angular-correlations and linear-polarization analysis indicates spin-parity of 6^+ for the 4292.1-keV level in ^{98}Zr. This assignment is further supported by γ decays of the 4292.1-keV level to the 4^+ levels at 1843.4 and 2047.7 keV. Furthermore, the 4292.1-keV level is populated very weakly, if at all, in fission of ^{248}Cm and ^{252}Cf, indicating its rather non-yrast character. In the β^- decay of ^{98}Y we also observe the population of the 4545.5-keV level with a tentative spin assignment of (7^+). Finally, the decay of the 2.36-s isomer in ^{98}Y has a 43% branch to the 4292.1-keV level, consistent with an allowed G-T transition, only. All these observations indicate spin-parity $I = (6,7)^+$ for the 2.36-s isomer in ^{98}Y. In the case where the spin of the 2.36-s isomer is 6^+, the single-particle rate of the unobserved 90.6-keV, $M2$ decay to the 375.1-keV level corresponds to a half-life of 10^{-4} s. Therefore, spin 7^+ is more likely, because then the transition is an $E3$, the corresponding half-life is about 5 s and the total conversion coefficient is 15.5, matching well the experimental hindrances.

With spin-parity 7^+ the structure of the isomer has to involve the $g_{9/2}$ proton. On the neutron side the $d_{5/2}$ or $g_{7/2}$ orbitals may contribute, producing an $I^\pi = 7^+$ spherical configuration. However, the spherical shape is in conflict with the large deformation reported for the isomer in Ref. [9]. Another intriguing observation is the low population of the 2.36-s isomer, which is about 0.1 of the population of the 4^- isomer at 496.1 keV. This suggests an exotic structure of the 2.36-s isomer.

The involvement of the $9/2^+[404]$ neutron extruder orbital may provide a solution. The $9/2^+[404]$ extruder was first proposed by Meyer *et al.* [60] in ^{99}Y in the $(\pi 5/2^+[422], \nu 9/2^+[404]\nu 3/2^+[411])_{11/2^+,17/2^+}$ configurations, assigned to the 1.4-ns and 8.6-μs isomers, respectively. The $\nu 9/2^+[404]$ extruder was later observed directly at low excitation energies in ^{99,101}Zr and ^{97}Sr [4,5,20,61]. Its role in creating deformed configurations in the region was discussed in Refs. [4,5]. For the 2.36-s isomer in ^{98}Y we propose the $(\pi 5/2^+[422], \nu 9/2^+[404])_{7^+}$ configuration, the one which contributes to the three-quasiparticle isomers in ^{99}Y. This solution agrees with the large deformation of the isomer in ^{98}Y [9].

The remaining problem is the nonobservation of any deformed band on top of the 2.36-s isomer, expected here due to its high deformation [9]. The QPRM calculations performed in this work predict the deformed $(\pi 5/2^+[422], \nu 9/2^+[404])_{7^+}$ configuration at low excitation energy. The rotational band calculated on top of this level involves $M1 + E2$ transitions with energies of 274, 311, 347,... keV. From the point of view of the population in fission, the band on top of the $I = 7$ band head is, effectively, shorter and less yrast than the cascade on top of the 4^- isomer, which would explain its apparent low population.

Finally, the $I = 7$ spin of the isomer suggests that the dynamic contribution to the deformation of the isomer is even larger than reported in Ref. [9]. This intriguing effect is discussed in more detail in Ref. [62], where an analogous isomer in ^{100}Y is reported. We note that the isomer in ^{100}Y has spin-parity 4^+ and the $\pi 5/2^+[422], \nu 3/2^+[411])_{4^+}$ configuration. Therefore, the effect is not associated with the proposed $\nu 9/2^+[404]$ extruder orbital.

B. β^- decay of ^{98}Y

The β^- decay of ^{98}Y is dominated by two Gamow-Teller transitions: one from the 0^- ground state to the 1^- level at 4165.2 keV ($\log_{10} ft = 4.2$) and the other from the 2.36-s isomer to the 6^+, 4292.1-keV level ($\log_{10} ft = 4.9$). The G-T transitions in this region correspond to the decay of the $g_{7/2}$ neutron to the $g_{9/2}$ proton, which therefore has to be incorporated in the structures of the involved levels.

1. β^- decay of the ground state

For the 4165.2-keV level no configuration has been proposed so far. The present analysis of angular correlations and linear polarization indicates spin-parity 1^- for the 4165.2-keV level. The $\log_{10} ft = 4.2$ value to this level from the 0^- ground state of ^{98}Y supports this assignment.

The $(\pi p_{1/2}, \nu s_{1/2})_{0^-}$ configuration of the ground state of ^{98}Y implies a decay of a neutron from the $(g_{7/2})^2_{0^+}$ pair in the ^{96}Sr core. This will produce in ^{98}Zr the $[(\pi g_{9/2}, \nu g_{7/2})_{1^+} \otimes (\pi p_{1/2}, \nu s_{1/2})_{0^-}]_{1^-}$, four-quasi-particle, spherical state, which may be expected at an excitation energy of 4.2 MeV. The dominating $E1$ decays from the 4165.2-keV level are probably enhanced by strong octupole coupling, present in this region, as found in the study of ^{96}Zr [46]. Analogous decays were observed in our recent study of mass $A = 86$ [27]. We note that the fast G-T transition ($\log_{10} ft = 4.2$) indicates rather pure spherical configurations involved in the decay.

2. β^- decay of the 2.36-s isomer

To the 8^+ spherical isomer at 1140 keV in ^{96}Y [57] the $(\pi g_{9/2}, \nu g_{7/2})_{8^+}$ configuration was assigned [46,52]. The isomer decays by the $\nu g_{7/2} \rightarrow \pi g_{9/2}$ G-T transition to the 8^+ spherical level at 4389.8 keV in ^{96}Zr having the $(\pi g^2_{9/2})_{8^+}$ configuration [46,63]. In the semimagic ^{96}Zr, the $(\pi g^2_{9/2})_{8^+}$, two-quasiparticle (2-q.p.) level may be expected at such high excitation energy.

In ^{98}Y the picture is different. The 465.7-keV isomer has lower spin and is strongly deformed [9]. Furthermore, the 6^+ level at 4292.1 keV in ^{98}Zr is also deformed, as suggested by the high population of the 4292.1-keV level in the decay of the deformed 465.7-keV isomer. Moreover, in ^{96}Sr and ^{98}Sr there are analogous 6^+, levels observed at 3604.2 keV [1] and 2533.1 keV [64], respectively. Both are deformed, as shown by rotational cascades on top of them. For the 6^+ level at 2533.1 keV in ^{98}Sr the 2-q.p. $(\nu 9/2^+[404], \nu 3/2^+[411])_{6^+}$ configuration was proposed [64], which is the G-M partner to the 2-q.p. $(\nu 9/2^+[404], \nu 3/2^+[411])_{3^+}$ configuration proposed for the 1837.3-keV level in ^{98}Sr [64,65]. The $\nu 9/2^+[404]$ orbital is well evidenced here. Therefore, it is likely that the $(\nu 9/2^+[404], \nu 3/2^+[411])_{6^+}$ deformed configuration

contributes to the wave function of the 4292.1-keV level in ^{98}Zr. The recent prompt-γ study of ^{98}Zr, populated in the cold-neutron-induced fission of ^{235}U, measured with EXILL, indicates the possible rotational band on top of the 4292.1-keV level [66]. The higher excitation energy of the 6^+, 4292.1-keV level in ^{98}Zr, as compared to the excitation energy of the 6^+, 3604.2-keV level in the ^{96}Sr isotone, is consistent with the $\nu 9/2^+[404]$ level being observed at higher energy in ^{99}Zr than in ^{97}Sr [5].

It is not clear whether the discussed 6^+ levels, which are significantly higher in energy than the discussed, 2-q.p. levels in ^{98}Sr, have a 2-q.p. or a 4-q.p. nature. The $(\nu 9/2^+[404], \nu 3/2^+[411])_{6^+}$ configuration involved in the wave function of the 4292.1-keV level means that it is not the $\nu 9/2^+[404]$ neutron of the $(\pi 5/2^+[422], \nu 9/2^+[404])_{7^+}$ isomeric structure in ^{98}Y which decays. We propose, therefore, that the 4292.1-keV level in ^{98}Zr has the 4-q.p. configuration $[(\pi 5/2^+[422], \nu 9/2^+[404])_{7^+} \otimes (\pi 7/2^+[413], \nu 5/2[413])_{1^+}]_{6^+}$, resulting from coupling the $(\pi 5/2^+[422], \nu 9/2^+[404])_{7^+}$ configuration of the 465.7-keV isomer in ^{98}Y to the $(\pi 7/2^+[413], \nu 5/2[413])_{1^+}$ product of the G-T decay of a neutron from a $(g_{7/2})^2_{0^+}$, deformed pair in the ^{96}Sr core. The high energy of the $\pi 7/2^+[413]$ proton orbital would explain the high excitation of the 6^+ level in ^{98}Zr.

One may also propose an alternative G-T transition, $(\nu 3/2[411]^2)_{0^+} \rightarrow (\pi 5/2^+[422], \nu 3/2[411])_{1^+}$, after which the $\pi 5/2^+[422]$ proton couples with the same proton of the 465.7-keV isomer configuration to $(\pi 5/2^+[422])^2_{0^+}$, leaving the $(\nu 9/2^+[404], \nu 3/2^+[411])_{6^+}$ 2-q.p. configuration for the 4292.1-keV level.

Both decays of the isomer to the 4292.1-keV level proposed above are more complex than the decay of the ground state of ^{98}Y to the 4165.2-keV level. This may explain the lower ($\log_{10} ft = 4.9$) rate of the corresponding G-T transition.

Although the question of whether the 4292.1-keV level is 2-q.p. or 4-q.p. is left for further studies, one can nevertheless conclude that the proposed structure of the 456.7-keV isomer is the first evidence of the $9/2^+[404]$ extruder in an odd-odd nucleus. It is also likely that a special type of the shape coexistence is observed in the ^{96}Sr core, where both spherical and deformed pairs of $g_{7/2}$ neutrons contribute to ^{98}Y $\rightarrow$ ^{98}Zr G-T transitions.

In the IBFFM calculations [52] the $\nu g_{9/2}$ orbital was considered unimportant. This was, however, after the authors pushed it 1.5 MeV away from the Fermi surface. Also the recent Monte Carlo Shell Model (MCSM) calculations [10] have not considered the $\nu 9/2^+[404]$ extruder, which seems to play an important role in creating nuclear deformation in the region.

V. SUMMARY

Excited states in ^{98}Y, populated in spontaneous fission of ^{248}Cm and ^{252}Cf and in neutron-induced fission of ^{235}U, were studied using the Eurogam2, Gammasphere, and EXILL Ge arrays and the Lohengrin fission-fragment separator of the ILL Grenoble. In ^{98}Y we found a deformed isomer with $T_{1/2} = 180(7)$ ns and a rotational band on top of it and a spherical isomer with $T_{1/2} = 0.45(15)\mu$s, analogous to the 8^+ isomer in ^{96}Y, corresponding to the $(\nu g_{7/2}, \pi g_{9/2})_{8^+}$ spherical configuration. An accurate excitation energy of 465.7(7) keV was measured using the JYFLTRAP Penning trap and a precise half-life of 2.36(6) s was determined for the long-lived 2.36-s isomer in ^{98}Y. We also studied excited levels in ^{98}Zr, populated following the β^- decay of the 2.36-s isomer to determine its configuration. The spin of the isomer was increased from the previous $I = (4,5)$ to $I^\pi = (6,7)^+$. The properties of this isomer suggest the presence of the $9/2^+[404]$ neutron extruder orbital in its structure, which can explain the large deformation of the isomer. This is the first observation of the $\nu 9/2^+[404]$ extruder orbital in an odd-odd nucleus.

Further studies of ^{98}Y are needed to confirm the spins of 465.7-, 496.1-, and $(564.0 + X)$-keV isomers. It is also important to identify the expected deformed band on top of the 465.7-keV isomer as well as the decay pattern of the $(564.0 + X)$-keV isomer.

The present work does not provide arguments to support the special role of the $\nu g_{7/2}$ - $\pi g_{9/2}$ interaction (the spin-orbit-partner, or SOP, mechanism) stressed in recent calculations. The rich, unique structure of ^{98}Y deserves new, dedicated calculations, testing the role of the $\nu 9/2^+[404]$ extruder identified in this nucleus, which was not considered in other calculations so far.

ACKNOWLEDGMENTS

This work has been supported by the Polish National Science Centre under Contract No. DEC-2013/09/B/ST2/03485. This material is based upon work supported by the U.S. Department of Energy, Office of Nuclear Physics, under Contract No. DE-AC02-06CH11357. The authors are indebted for the use of ^{248}Cm to the Office of Basic Energy Sciences, U.S. Dept. of Energy, through the transplutonium element production facilities at the Oak Ridge National Laboratory. This work has been supported by the Academy of Finland via the Finnish Centre of Excellence programs 2006-2011 and 2012-2017. The authors thank the technical services of the ILL, LPSC, and GANIL for supporting the EXILL campaign. The EXOGAM Collaboration and the INFN Legnaro are acknowledged for the loan of Ge detectors.

[1] W. Urban, J. L. Durell, A. G. Smith, W. R. Phillips, M. A. Jones, B. J. Varley, T. Rząca-Urban, I. Ahmad, L. R. Morss, M. Bentaleb, and N. Schultz, Nucl. Phys. A **689**, 605 (2001).

[2] T. Werner, J. Dobaczewski, M. W. Guidry, W. Nazarewicz, and J. A. Sheikh, Nucl. Phys. A **578**, 1 (1994).

[3] J. Skalski, S. Mizutori, and W. Nazarewicz, Nucl. Phys. A **617**, 282 (1997).

[4] W. Urban, J. A. Pinston, T. Rząca-Urban, A. Złomaniec, G. Simpson, J. L. Durell, W. R. Phillips, A. G. Smith, B. J. Varley, I. Ahmad, and N. Schulz, Eur. Phys. J. A **16**, 11 (2003).

[5] W. Urban, J. A. Pinston, J. Genevey, T. Rząca-Urban, A. Złomaniec, G. Simpson, J. L. Durell, W. R. Phillips, A. G. Smith, B. J. Varley, I. Ahmad, and N. Schulz, Eur. Phys. J. A **22**, 241 (2004).

[6] G. Lhersonneau, B. Pfeiffer, K.-L. Kratz, T. Enqvist, P. P. Jauho, A. Jokinen, J. Kantele, M. Leino, J. M. Parmonen, H. Penttilä, J. Äystö, and the ISOLDE Collaboration, Phys. Rev. C **49**, 1379 (1994).

[7] R. A. Meyer, E. A. Henry, and K. Heyde, Phys. Lett. B **177**, 271 (1986).

[8] J. A. Pinston, J. Genevey, R. Orlandi, A. Scherillo, G. S. Simpson, I. Tsekhanovich, W. Urban, H. Faust, and N. Warr, Phys. Rev. C **71**, 064327 (2005).

[9] B. Cheal, M. D. Gardner, M. Avgoulea, J. Billows, M. L. Bissell, P. Campbell, T. Eronen, K. t. Flanagan, D. H. Forest, J. Huikari, A. Jokinen, B. A. Marsh, I. D. Moore, A. Nieminen, H. Penttilä, S. Rinta-Antila, B. Tordoff, G. Tungate, and J. Äystö, Phys. Lett. B **645**, 133 (2007).

[10] T. Togashi, Y. Tsunoda, T. Otsuka, and N. Shimizu, Phys. Rev. Lett. **117**, 172502 (2016).

[11] C. Kermer, S. Aslanidou, S. Bassauer, M. Hilcker, A. Krugmann, P. von Neumann-Cosel, T. Otsuka, N. Pietralla, V. Yu. Ponomarev, N. Shimizu, M. Singer, G. Steinhilber, T. Togashi, Y. Tsunoda, V. Werner, and M. Zweidinger, Phys. Rev. Lett. **117**, 172503 (2016).

[12] B. Singh and Z. Hu, Nucl. Data Sheets **98**, 335 (2003).

[13] P. J. Nolan, F. A. Beck, and D. B. Fossan, Annu. Rev. Nuc. Part. Sci. **44**, 561 (1994).

[14] W. Urban, M. A. Jones, C. J. Pearson, I. Ahmad, M. Bentaleb, J. L. Durell, M. J. Leddy, E. Lubkiewicz, L. R. Morss, W. R. Phillips, N. Schulz, A. G. Smith, and B. J. Varley, Nucl. Instrum. Methods A **365**, 596 (1995).

[15] T. Rząca-Urban, W. R. Phillips, J. L. Durell, W. Urban, B. J. Varley, C. J. Pearson, J. A. Shannon, I. Ahmad, C. J. Lister, L. R. Morss, K. L. Nash, C. W. Williams, M. Bentaleb, E. Lubkiewicz, and N. Schulz, Phys. Lett. B **348**, 336 (1995).

[16] W. Urban, M. A. Jones, J. L. Durell, M. J. Leddy, W. R. Phillips, A. G. Smith, B. J. Varley, I. Ahmad, L. R. Morss, M. Bentaleb, E. Lubkiewicz, and N. Schulz, Nucl. Phys. A **613**, 107 (1997).

[17] W. Urban, W. R. Phillips, J. L. Durell, M. A. Jones, M. Leddy, C. J. Pearson, A. G. Smith, B. J. Varley, I. Ahmad, L. R. Morss, M. Bentaleb, E. Lubkiewicz, and N. Schulz, Phys. Rev. C **54**, 945 (1996).

[18] D. Patel, A. G. Smith, G. S. Simpson, R. M. Wall, J. F. Smith, O. J. Onakanmi, I. Ahmad, J. P. Greene, M. P. Carpenter, T. Lauritsen, C. J. Lister, R. F. Janssens, F. G. Kondev, D. Seweryniak, B. J. P. Gall, O. Dorveaux, and B. Roux, J. Phys. G. Nucl. Part. Phys. **28**, 649 (2002).

[19] E. Moll, H. Schrader, G. Siegert, H. Hammers, M. Asghar, J. P. Bouget, P. Armbruster, H. Ewald, and H. Wollnik, Kerntechnik **19**, 374 (1977).

[20] A. Złomaniec, H. Faust, J. Genevey, J. A. Pinston, T. Rząca-Urban, G. S. Simpson, I. Tsekhanovich, and W. Urban, Phys. Rev. C **72**, 067302 (2005).

[21] B. Singh, Nucl. Data Sheets **84**, 565 (1998).

[22] H. Mach and R. L. Gill, Phys. Rev. C **36**, 2721 (1987).

[23] B. Pfeiffer (private communication).

[24] Y. Zheng, G. de France, E. Clement, A. Dijon, B. Cederwall, R. Wadsworth, T. Bäck, F. Ghazi Moradi, G. Jaworski, B. M. Nyako *et al.*, Phys. Rev. C **87**, 044328 (2013).

[25] P. Mutti *et al.*, in Proceedings of the International Conference ANIMMA 2013, Marseille, France (unpublished); A. Blanc *et al.*, EPJ Web Conf. **62**, 01001 (2013).

[26] M. Jentschel, A. Blanc, G. de France, U. Köster, S. Leoni, P. Mutti, G. Simpson, T. Soldner, C. Ur, W. Urban *et al.*, J. Instrum. (to be published).

[27] W. Urban, K. Sieja, T. Materna, M. Czerwiński, T. Rząca-Urban, A. Blanc, M. Jentschel, P. Mutti, U. Köster, T. Soldner, G. de France, G. S. Simpson, C. A. Ur, C. Bernards, C. Fransen, J. Jolie, J.-M. Regis, T. Thomas, and N. Warr, Phys. Rev. C **94**, 044328 (2016).

[28] P. M. Jones, L. Wei, F. A. Beck, P. A. Butler, T. Byrski, G. Duchêne, G. de France, F. Hannachi, G. D. Jones, and B. Kharraja, Nucl. Instrum. Methods A **362**, 556 (1995)

[29] G. Audi, O. Bersillon, J. Blachot, and H. Wapstra, Nucl. Phys. A **729**, 3 (2003).

[30] G. Audi and H. Wapstra, Nucl. Phys. A **595**, 409 (1995).

[31] T. Eronen, V. S. Kolhinen, V.-V. Elomaa, D. Gorelov, U. Hagerc, J. Hakala, A. Jokinen, A. Kankainen, P. Karvonen, S. Kopecky, I. D. Moore, H. Penttilä, S. Rahamane, S. Rinta-Antila, J. Rissanen, A. Saastamoinen, J. Szerypo, C. Weber, and J. Äystö, Eur. Phys. J. A **48**, 46 (2012).

[32] T. Eronen, V.-V. Elomaa, U. Hager, J. Hakala, A. Jokinen, A. Kankainen, S. Rahaman, J. Rissanen, and C. Weber, and J. Äystö, Nucl. Instrum. Methods B **266**, 4527 (2008).

[33] S. George, K. Blaum, F. Herfurth, A. Herlert, M. Kretzschmar, S. Nagy, S. Schwarz, L. Schweikhard, and C. Yazidjian, Int. J. Mass Spectrometry **264**, 110 (2007).

[34] A. Kellerbauer, K. Blaum, G. Bollen, F. Herfurth, H.-J. Kluge, M. Kuckein, E. Sauvan, C. Scheidenberger, and L. Schweikhard, Eur. Phys. J. D **22**, 53 (2003).

[35] M. Wang, G. Audi, A. H. Wapstra, F. G. Kondev, M. MacCormick, X. Xu, and B. Pfeiffer, Chin. Phys. C **36**, 1603 (2012).

[36] J. K. Hwang, A. V. Ramayya, J. Gilat, J. H. Hamilton, L. K. Peker, J. O. Rasmussen, J. Kormicki, T. N. Ginter, B. R. S. Babu, C. J. Beyer *et al.*, Phys. Rev. C **58**, 3252 (1998).

[37] M. Ramdhane, G. S. Simpson, F. Drouet, T. Malkiewicz, A. Vancraeyenest, C. Gey, P. Alexa, G. Thiamova, G. Kessedjian, C. Sage *et al.*, Acta Phys. Pol. B **47**, 911 (2016).

[38] W. Urban, K. Sieja, G. S. Simpson, H. Faust, T. Rząca-Urban, A. Złomaniec, M. Łukasiewicz, A. G. Smith, J. L. Durell, J. F. Smith, B. J. Varley, F. Nowacki, and I. Ahmad, Phys. Rev. C **79**, 044304 (2009).

[39] Ł. W. Iskra, B. Fornal, S. Leoni, G. Bocchi, A. Petrovici, C. Porzio, A. Blanc, G. de France, M. Jentschel, U. Köster, P. Mutti, J.-M. Regis, G. Simpson, T. Soldner, C. A. Ur, W. Urban, D. Bazzacco, G. Benzoni, S. Bottoni, A. Bruce, N. Cieplicka-Orynczak, F. C. L. Crespi, L. M. Fraile, W. Korten, T. Kröll, S. Lalkovski, N. Marginean, C. Michelagnoli, B. Melon, D. Mengoni, B. Million, A. Nannini, D. Napoli, Zs. Podolyak, P. H. Regan, and B. Szpak, Europhys. Lett. **117**, 12001 (2017).

[40] Ł. W. Iskra, G. Bocchi, B. Fornal, S. Leoni, S. Bottoni, N. Cieplicka-Orynczak, M. Jentschel, U. Köster, C. Michelagnoli, P. Mutti, T. Soldner, A. Blanc, G. de France, G. Simpson, C. A. Ur, and W. Urban, Acta Phys. Pol. B **48**, 581 (2017).

[41] G. Lhersonneau, D. Weiler, P. Kohl, H. Ohm, K. Sistemich, and R. A. Meyer, Z. Phys. A **323**, 59 (1986).

[42] A. A. Sonzogni, Nucl. Data Sheets **103**, 1 (2004).

[43] G. Audi, F. G. Kondev, Meng Wang, W. J. Huang, and S. Naimi, Chin. Phys. C **41**, 030001 (2017).

[44] T. Kibédi, T. W. Burrows, M. B. Trzhaskovskaya, P. M. Davidson, and C. W. Nestor Jr., Nucl. Instr. Meth. A **589**, 202 (2008); http://bricc.anu.edu.au/.
[45] K. Becker, G. Jung, K.-H. Kobras, and H. Wollnik, and B. Pfeiffer, Z. Phys. A **319**, 193 (1984).
[46] M. L. Stolzenwald, S. Brant, H. Ohm, K. Sistemich, and G. Lhersonneau, in *Proceedings of the International Workshop on Nuclear Structure of the Zirconium Region, Bad Honnef, Germany, 24–28 April 1988*, edited by J. Eberth, R. A. Meyer, and K. Sistemich, Research Reports in Physics (Springer-Verlag, Berlin, 1988), p. 239.
[47] www.nndc.bnl.gov/logft/.
[48] K. S. Krane, R. M. Steffen, and R. M. Wheeler, Nucl. Data Tables **11**, 351 (1973).
[49] *The Electromagnetic Interaction in Nuclear Spectroscopy*, edited by W. D. Hamilton (North-Holland, Amsterdam, 1975).
[50] U. Hager, A. Jokinen, V.-V. Elomaa, T. Eronen, J. Hakala, A. Kankainen, S. Rahaman, J. Rissanen, I. D. Moore, S. Rinta-Antila, A. Saastamoinen, T. Sonoda, and J. Äystö, Nucl. Phys. A **793**, 20 (2007).
[51] I. Ahmad and W. R. Phillips, Rep. Prog. Phys. **58**, 1415 (1995)
[52] S. Brant, G. Lhersonneau, and K. Sistemich, Phys. Rev. C **69**, 034327 (2004).
[53] W.-W. Muller, Nucl. Data Sheets **39**, 467 (1983).
[54] L. K. Peker, F. K. Wohn, J. C. Hill, and R. F. Petry, Phys. Lett. **B169**, 323 (1986).
[55] S. Brant, G. Lhersonneau, M. L. Stolzenwald, and K. Sistemich, Z. Phys. A **329**, 301 (1988).
[56] P. Alexa, J. Kvasil, N. V. Minh, and R. K. Sheline, Phys. Rev. C **55**, 179 (1997).
[57] D. Abriola and A. A. Sonzogni, Nucl. Data Sheets **109**, 2501 (2008).
[58] P. Federman and S. Pittel, Phys. Lett. B **69**, 385 (1977); **77**, 29 (1978); Phys. Rev. C **20**, 820 (1979).
[59] P. Federman, S. Pittel, and R. Campos, Phys. Lett. B **82**, 9 (1979).
[60] R. A. Meyer, E. Monnand, J. A. Pinston, F. Schussler, I. Ragnarsson, B. Pfeiffer, H. Lawin, G. Lhersonneau, T. Seo, and K. Sistemich, Nucl. Phys. A **439**, 510 (1985).
[61] J. K. Hwang, A. V. Ramayya, J. H. Hamilton, D. Fong, C. J. Beyer, P. M. Gore, Y. X. Luo, J. O. Rasmussen *et al.*, Phys. Rev. C **67**, 054304 (2003).
[62] K. Baczynska, J. Billowes, P. Campbell, F. C. Charlwood, B. Cheal, T. Eronen, D. H. Forest, A. Jokinen, T. Kessler, I. D. Moore, M. Rffer, G. Tungate, and J. Äystö, J. Phys. G **37**, 105103 (2010).
[63] M. L. Stolzenwald, G. Lhersonneau, S. Brant, G. Menzen, and K. Sistemich, Z. Phys. A **327**, 359 (1987).
[64] J. L. Durell, T. J. Armstrong, and W. Urban, Eur. Phys. J. A **20**, 97 (2004).
[65] G. Lhersonneau, B. Pfeiffer, K.-L. Kratz, H. Ohm, K. Sistemich, S. Brant, and V. Paar, Z. Phys. A **337**, 143 (1990).
[66] S. Mukhopadhyay, D. C. Biswas, L. S. Danu, A. K. Kumawat, A. Singh, A. Blanc, G. de France, M. Jentschel, U. Köster, S. Leoni, P. Mutti, G. S. Simpson, T. Soldner, C. A. Ur, and W. Urban, in Proceedings of the DAE-BRNS Symposium on Nuclear Physics 2016, Kolkata, India (unpublished).